OCCASION

This publication has been made available to the public on the occasion of the 50th anniversary of the United Nations Industrial Development Organisation.

DISCLAIMER

FAIR USE POLICY

CONTACT

Please contact publications@unido.org for further information concerning UNIDO publications.

For more information about UNIDO, please visit us at www.unido.org

UNITED NATIONS INDUSTRIAL DEVELOPMENT ORGANIZATION
Vienna International Centre, P.O. Box 300, 1400 Vienna, Austria
Tel: (+43-1) 26026-0 · www.unido.org · unido@unido.org

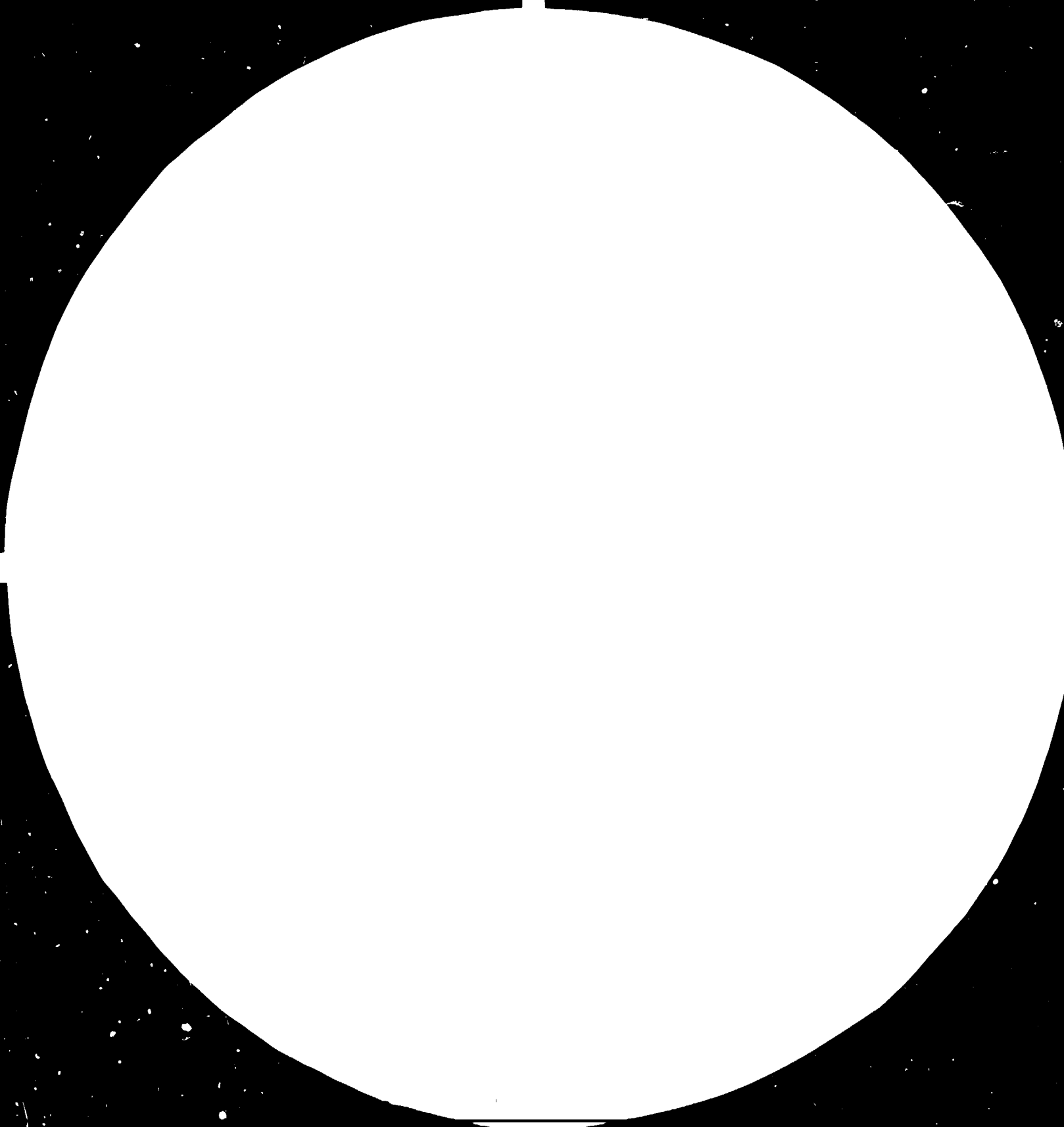

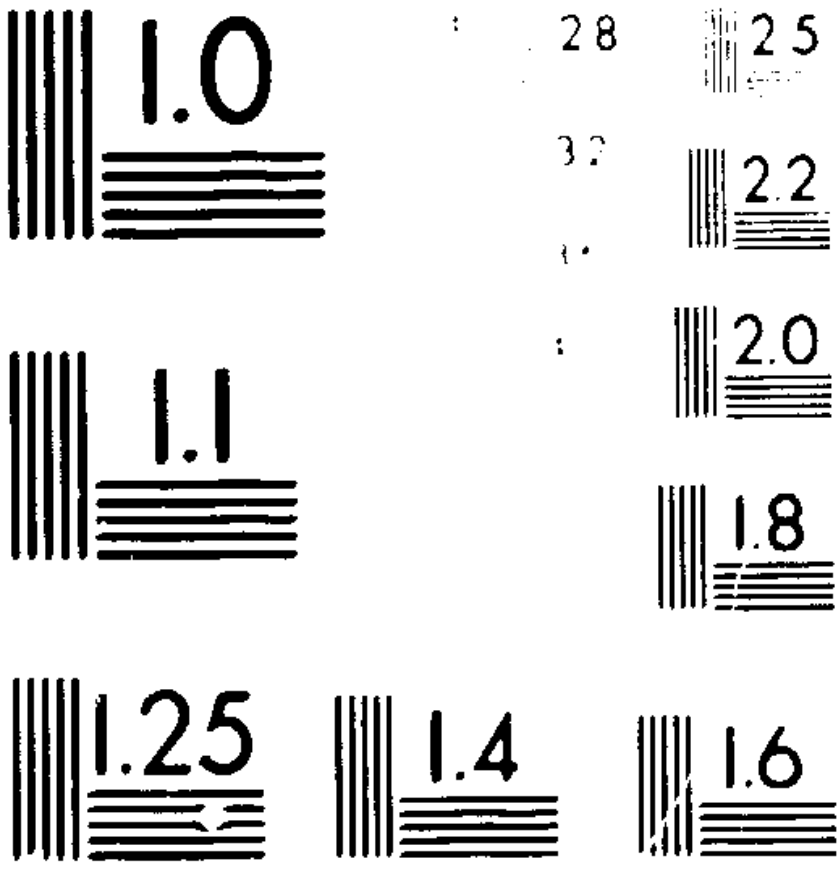

13545

Distr.
LIMITED

ID/WG.416/11
2 February 1984

ENGLISH

United Nations Industrial Development Organization

International Conference on
Carbon Fibre Applications

São José dos Campos, Salvador, Brazil,
5-9 December 1983

MECHANISMS OF FRACTURE IN FIBRE REINFORCED STRUCTURES*

by

Heinrich W. Bergmann**

* The views expressed in this paper are those of the author and do not necessarily reflect the views of the secretariat of UNIDO. This document has been reproduced without formal editing.

** Deutsche Forschungs- und Versuchsanstalt für Luft- und Raumfahrt (DFVLR), Postfach 3267, 3300 Braunschweig, F.R.G.

V.84-81164

Summary

Structures composed of fiber-reinforced materials may exhibit various kinds of defects incurred in the manufacturing process or during service. The ability to forecast the effects of such defects on the safe operation of aerospace structures presupposes the development of principles of defect mechanics, analogous to fracture mechanics but considerably more complex. Following the identification of potential failure modes, the judgment of their contribution to the progression of observed defects requires extended empirical and analytical investigations. Unless the mechanisms of defect progression are understood and predictable, the disposition of an afflicted structure must be supported by costly and time-consuming tests. The ultimate goal, therefore is the translation of the many complicated relationships into reliable and relatively simple accept/reject/repair criteria for the support of series production and maintenance requirements. The related activities of the DFVLR Institut for Structural Mechanics are guided by this goal. The present paper does not purport to offer simple solutions; rather, it aims to convey the complexity of the issue of damage mechanics.

1. Introduction

The concept of fiber-reinforced materials is not new and certainly not an invention of this century. However, only in recent years has the development of special fibers, in combination with appropriate matrix materials, led to promising applications in the aerospace industry. Of dominant interest are carbon-fiber reinforced epoxy resins which, apart from their high specific strength and stiffness properties, are also fatigue-tolerant and corrosion-resistant.

Inhibiting a wider range of applications are the small elongations to failure of epoxy resins, their susceptibility to environmental effects, and an as yet insufficient comprehension of the significance of defects occuring during the production process of structural parts, or in the course of their service. The disposition of such flaws as microcracks, delaminations, misdrilled holes, etc., by analytical means, in general, is as yet impossible for a lack of understanding of the mechanisms of damage progression. Consequently, the accept/reject decisions of damaged parts are normally made by time-consuming testing and often after extensive repairs. The knowledge thus gained is seldom transferable as it provides no insight into the interdependence of the many parameters affecting the response of damaged parts.

Anticipating a rapid increase of composite structures in the near future, the issue of damage mechanics was introduced as a major research program at the Institute for Structural Mechanics of the German Aerospace Research Establishment (DFVLR). It is fully recognized that the complexitiy of damage mechanics exceeds that of facture mechanics by far, partially because of the anisotropy and heterogeneity of the composite material, and partially because of the much larger variety of possible kinds of damage.

2. Test Program

Considering the large variety of parameters to be encountered, it stood to reason to commence the experimental investigations with standard tape prepregs for autoclave curing. The dominantly used material is 914C/T300; all subsequent statements relate to that material unless otherwise noted.

The stacking orders of the laminates are chosen such that they represent rib or spar chords, webs and skin panels of aerospace structures. For the purpose of comparing their performance, test specimens are prepared without defects and with typical defects such as delaminations, notches, microcracks, etc. The majority of the test specimens for tension and compression tests correspond to the dimensions given in Figure 1. The substantial width of the larger specimens assures that the response of the centrally introduced defects is unaffected by the specimen boundaries. Under compression loading the test specimens must be laterally supported by anti-buckling guides. In cyclic-tests the specimen temperature may rise significantly due to internal and external friction and in dependance on the test frequency. In order to control the temperature effect the anti-buckling guides contain electrically activated cooling devices. The test specimens are loaded under realistic environmental conditions including moisture, temperature and radiative effects. Test extend to eventual failure under increasing static loads as well as under cyclic loads.

3. Failure Analysis

In carbonfiber-reinforced laminates, different specimen configurations and different loading and environmental conditions lead to different failure modes. The dependency of the micro-failure modes, especially, on the many possible parameter combinations is as yet not well understood. In fact in may be said that the investigation, classification and interpretation of failure modes is still in its infancy.

The failure analysis techniques currently existing are: microscopic examinations from which the nature, origin and propagation direction of some flaws may be deduced; non-destructive evaluations for the detection and monitoring of macroscopic types of damage; and stress analysis of failed test specimens or structural components.

3.1 Microscopic Examinations

Failure modes observable on the microscopic scale include fiber pullout, fiber breakage, matrix micro-cracking, fiber-matrix debonding, and matrix deformations in the form of serrations and cleavage. Their subsequent progression will eventually cause fracture of the whole laminate. Fractographic techniques based on scanning electron beam microscopy can be applied to identify the fracture origin and the direction of propagation, as well as to analyse material parameters affecting the fracture process, such as constituent properties, laminate configurations, fiber-matrix interface properties, loading and environmental conditions. A reliable characterization of the fracture phenomena may ultimately assist in establishing the cause of failure and thus suggest suitable modifications of the composite system.

3.2 Nondestructive Evaluation

Non-destructive evaluations of all test specimens is mandatory in order to assure the absence of initial damage and to detect and track the various kinds of defects. As no single procedure can satisfy this requirement, a combination of mutually supportive procedures must be employed. The techniques the utilized by the Institute for Structural Mechanics include a) high-precision ultrasonic test facilities with highly-vaporated focussing transducers and a narrowband transmitter with variable pulse frequency; b) low-energy X-ray equipment with high lateral resolution; c) acoustic emission analysis and a grid-reflection technique for in-situ observations of the test specimens.

3.3 Stress Analysis

A reasonably accurate analysis of the three-dimensional state of stress around a discontinuity by a standard finite-element approach would require such a large number of degrees of freedom that the solutions would soon become prohibitively expensive, especially when the tracking of the damage progression involves an iterative treatment or when, perhaps additionally, non-linear effects need to be included. This recognition has led to the development of a new analysis approach which, conceptually, is not novel but which combines an unusual number of features in an economically organized computer program.

Its basic component is a triangular hybrid shell element comprising bending and membrane action as well as response to surface tractions on this upper and lower surfaces. By stacking several of these elements above one another, a laminate can be modelled in great detail with a reasonably small number of degrees of freedom. A special condensation scheme is utilited to produce multilayer shell elements and substructures. Failure progression rules are appended to the finite element equation system in such a way that tracing of damage progression will not require repeated triangularization of the global stiffness matrix.

4. Mechanisms of Fracture

In contrast to metals, where fracture under static or fatigue loads results from the nucleation and growth of a single dominant flaw, the fracture of fiber-reinforced composites is characterized by initiation and progression of multiple failures of different modes such as matrix cracks, interfacial debonding, fiber breaks and delaminations between adjacent plies of the laminates. The kinds of occuring failures, their distribution, time sequence and possible interactions depend on many parameters such as the properties of the fiber/matrix system, the stacking order and curing process, the influence of the environment, etc. The

problem is further complicated by the possibility of fatigue failure in the compressive as well as in the tensile load regime, and by different failure modes under static and dynamic load applications.

Even in the case of very closely controlled tension tests performed under identical parametric conditions the scatter of the test results is usually high, especially with respect to the fatigue life of the specimens. A possible explanation is that at sufficiently high stress levels the random distribution of microcracks, debonds, fiber breaks, etc. becomes increasingly denser. Toward the end of specimen life, adjacent failure modes interconnect and form complex failure paths which, because of their stochastic nature, differ from specimen to specimen and lead to discrepant life spans of the test specimens. A similar argument may apply to the fatigue performance of specimens subject to compressive loads where, of course, different kinds of failure modes interact differently but produce similarly scattered test results.

Close observation of unnotched specimens tested under cyclic tension loads indicates that the progression of events follows a more or less distinct pattern. The first discernable damage usually are microcracks at certain intervals in the crossplies of the laminates. With increasing cycles more microcracks develop which, at the interfaces with neigboring plies, tend to turn and to form small delaminations both inside and, especially, at the free edges of the laminate. Additional delaminations emanate from the locations of fiber or fiber bundle breaks and lead to a damage state depicted in Figure 2.

With respect to compressive loads, critical conditions may arise in the presence of delaminations induced by preceding high tensile loads, by lack of adhesion because of faulty manufacturing, or because of impact damage. Under sufficiently high compressive stresses the reduced stiffness of the separated sections will invite their buckling and thereby induce

a state of stress at the periphery of the delamination which tends to advance the crack front. Continuation of load cycling then leads to damage growth followed by massive separation and subsequent specimen failure.

Accompanying the gradually increasing damage state is a noticeable reduction of the overall laminate stiffness. Depending on the stacking order, this reduction may be as pronounced as shown in Figure 3 for a matrix-controlled $\left[\pm 45\right]_{2s}$-laminate, or as subtle as in the case of the fiber-controlled $\left[0_2,+45,0_2,-45,0,90\right]_s$-laminate shown in Figure 4. In both instances, however, a particularly critical combination of local failure modes develops finally which leads to a rapid deterioration of the stiffness in only a few additional cycles and to what is commonly called "sudden death" of the specimen.

4.1 Microcracks

The normally used epoxy resins exhibit very limited strain capabilities. In addition, the discrepant thermal expansions of the fibers and the resins induce adverse prestresses as a result of the curing process. Under these conditions the formation of microcracks can be expected in those plies of a laminate which are mechanically or thermally stressed beyond the critical strain values of the resin. Typical examples of microcracks observed radiographically in the crossplies of $\left[0,90\right]_s$-laminates during a tension test are shown in Figure 5.

Repeated exposures to high mechanical loads or to low temperatures will aggravate the state of damage. Figure 6 shows that in $\left[\pm 45\right]_{2s}$-specimens subjected to thermal cycles between $+100^{\circ}C$ and $-155^{\circ}C$ the cracks turn at the interfaces of adjacent plies and form local delaminations which tend to grow with increasing

numbers of thermal cycles. It stands to reason that a similar effect occurs in specimens subjected to sufficiently high mechanical load cycles. Delaminations of this kind occur most severely along the free edges but are found in the interior of the test specimens as well.

Considering that the strain value associated with the first crack in any one ply is often equated to the limit-load carrying capability of the structure, the urgent need for more ductile resin systems is self-evident.

4.2 Fiber Breaks and Fiber Debonds

Observable also on an initially microscopic level are failure modes such as fiber breaks and fiber debonds.

In highly stressed laminates fibers may rupture prematurely, individually or in small bundles, because of their imperfect shapes or imperfect alignment. Especially in fiber-controlled stacking orders the resulting redistribution of stresses in the vicinity of such discontinuities may initiate the type of local failure modes which affect the fracture behavior of the laminate. Figure 7 depicts the observation of the break of a fairly massive fiber bundle by the grid-reflection technique as well as the associated spalling and cracking of the affected zone.

The loss of adhesion between fiber and matrix is often referred to as debonding. The cause may be a locally faulty surface treatment, or the gradual deterioration of an initially good bond by mechanically or thermally induced fatigue. An example of latter is given in Figure 8,showing the fracture surfaces of tension-loaded specimens before and after severe thermal cycling. While prior to cycling the many specks of resin adhering to the fiber surfaces indicate a rasonably strong bond, the much smoother

surfaces after cycling seem to signal the loss of it. It may be expected that similar degradations take place under mechanical loads. As a consequence of progressive debonding, a gradual deterioration of the laminate stiffness might be expected. Figure 9 seems to lend credence to this argument although it is not clear to what extent additional cracking contributes to the stiffness degradation.

4.3 Edge Delaminations

The free edges of mulidirectional laminates are especially susceptible to the formation of cracks and delaminations because, under imposed axial strains, the enforced compatibility of the lateral contractions of the individual plies introduces interlaminar shearing stresses as well as normal stresses in the thickness direction. The resulting state of stress, shown schematically in Figure 10, depends on the stacking order and on the load direction. Figure 11 summarizes the results of a dedailed finite-element analysis for laminates stacked $[0,\pm45,90]_s$ and $[90,\pm45,0]_s$ The numerical values of the linearly derived stresses account neither for curing prestresses nor for viscoelastic relaxation; however, their potentially dangerous trends can apparently be reversed by altering the ply sequence. The question arises to what extent, and if at all, the actual strengths of the laminates is affected by such ply rearrangements. As the commonly used lamination theory does not account for these internal states of stress, equal strengths are predicted on that basis.

Carefully conducted static tension tests confirm, indeed, a superiority of the $[90,\pm45,0]_s$-laminate over the other by approximately 10 %. Apart from the reversed crossply locations, the developing microcrack patterns were comparable in both cases without noticeable evidence of edge delaminations.

A very different behavior of the two laminates was observed during fatigue loading with R=+0.1 and an upper stress level of 75 % of their respective static strengths. As expected, microcracking and edge delaminations occurred relatively early in the $[0,\pm45,90]_s$-specimens. Monitored by contrast-enhanced radiography, as shown in Figure 12, the delaminations proceeded from both sides toward the center of the specimen until, shortly before failure, they were separated only by the narrow strip recognizable in Figure 13. The $[90,\pm45,0]_s$- specimens, in contrast, exhibited relatively minor evidence of damage. The appearance of a typical free edge, shortly before failure, is shown in Figure 14. Incipient delaminations are recognizable between those plies where, according to Figure 11, the internal stresses are most severe.

In spite of the totally different kinds of fracture, the number of cycles to total failure was comparable for both types of laminates. Conceivably, the two separated halves of the $[0,\pm45,90]_s$-laminates were capable of maintaining the 75 % static strength level more or less independently. Sep-rations of this sort in tension-compression or purely compression-loaded specimens, of course, would reduce the fatigue life drastically because of buckling of the separated sections. The point here is that an evalution of test results alone, i.e. without an accompanying failure analysis, may lead to erroneous conclusions in regard to the performance characteristics of laminates.

Figure 15 shows a series of enlargements of the tip of an edge delamination of a $[0_2,+45,0_2,-45,0,90]_s$-laminate which convey an interesting impression of the crack pattern in the matrix material.

In actual applications the boundaries of structural components, such as panels, are often reinforced or less intensely stressed. The issue of edge effects, nevertheless, is of high significance as it also applies to the free boundaries of holes, notches or cutouts. More importantly even, as the design allowables are normally defined on the basis of narrow test specimens, a superficial interpretation of test results may entail overly conservative design values.

4.4 Central Delaminations

Apart from the free edges of a laminate, delaminations may occur in the central regions as a consequence of microcrack formation and growth, or because of local lack of adhesion between adjacent plies caused either by a processing fault or by impact damage during service. The response of such delaminations under static and cyclic loads is a major aspect of the damage mechanics program.

The introduction of delaminations in test specimens is possible by the inclusion of an outgassing agent or by the imbedment of a very thin teflon disk prior to curing, or by controlled impacting after curing. The former has the advantage of providing a well-defined location and geometry and has been adopted for the majority of the studies. Numerous tests have proven that the somewhat blunted crack front does not significantly retard the eventual growth of the delamination.

Figure 16 shows, by means of ultrasonic records, the progressive growth of a delamination under a gradually increasing compressive load in a standard test specimen. The 0.1 mm thick teflon disk was placed between the 90^{o}-plies at the midplane of the specimen. Up to approximately 85 % of ultimate load the delamination is seen to be stable to then grow in the direction of the fibers of the neighboring plies. The same kind of test specimen loaded in tension exbibits a very different behavior. Figure 17 shows that, while the central delamination remains unchanged up to failure of the specimen, edge delaminations occur along the free boundaries at approximately 80 % of ultimate load which subsequently gradually increase. Figure 18, finally, illustrates the response of a test specimen under cyclic load with R=-1 and a stress level of ca. 50 % of its ultimate strength. After 20000 cycles the first evidence of central delamination growth and onset of edge delaminations is noticeable, which gradually increase in severity until failure after 140000 cycles.

Figure 17 also indicates the formation and random distribution of an increasing number of local delaminations, not to be found under static loads and consistent with the argument offered in Section 2.

Variations of the diameter of the delaminations or of their location within their stacking order, obviously, will produce different results. Figure 19 summarizes some of the accumulated test data which indicate that the size of the delaminations is less significant than their location. A ready explanation is the increasing tendency of the thinner of the separated section to buckle out and to thereby aggravate the state of stress at the perimeter of the delamination.

The intent of the test program is to identify tolerance levels for delaminations below which no growth occurs, and to predict the rate of growth of delaminations above those tolerance levels by empirical/analytical procedures.

5. Environmental Effects

The influence of the environment on the strength and stiffness of epoxy resins is a well known phenomenon. Figure 20 shows, typically, the strength dependence of $[0,\pm45,0]$-laminates (Fiberite 934/T300) on both temperature and moisture. The degrading trends are reversible upon drying of the laminate and/or by lowering of the temperature. Potential damage can be inflicted, however, by thermal shocking or by sustained exposure to high temperatures. Figure 21 depicts the gradual loss of weight of epoxy laminates exposed to $100^{o}C$ and $120^{o}C$ for up to 2000 hours. The tests were performed under atmospheric conditions and produced no visible changes of the surface properties. Additional tests with neat resins in and out of vacuum traced the weight loss to an oxidative process accompanied by significant stiffness degradations.

A different kind of degradation occurs after prolonged exposure of epoxy laminates to ultraviolet radiation. According to Figure 22, a slight increase in strength, probably caused by postcuring of the resin, is followed by a gradual decrease as a consequence of the erosive deterioration of the laminate surfaces. As a point of interest it may be mentioned that epoxy laminates subjected to $3x10^{8}$ rads of electron radiation, in vacuum, did not suffer degradation in strength or stiffness although the laminate surfaces exhibited a slight reddish tint.

Apart from laminate strength and stiffness, elevated temperatures as well as moisture affect significantly the strain capability of the epoxy resin. Figure 23 depicts the microcrack formation along the free edges of $[0,90]_{s}$-laminates tension-loaded to failure under different temperature and moisture conditions. In the dry state, the diminishing number of cracks at increasing temperature signals a higher degree of ductility, while in the moist state the onset of cracking is retarded by the relieving superposition of the swelling strains on the curing strains. From the damage-mechanical point of view it es essential that such considerations enter into the analysis of failure modes.

6. Limits of Fracture Mechanics

The complexity of the failure modes of fiber-reinforced laminates makes an adoption or modification of established fracture-mechanical principles difficult or impossible. Exceptions, perhaps, are such simple cases as cracks parallel to the fibers of unidirectional laminates or delaminations between adjacent plies.

Even the classical problems of a drilled hole or an elongated notch prove to be elusive. Admittedly, several models based on fracture mechanics have been introduced for their pragmatic treatment, all based on the assumption that failure will occur when the crack tip damage reaches a critical value. This concept of critical damage zone size represents the complex crack tip damage as an "effective" crack length and stipulates that the damage growth can be modelled as a self-similar crack extension. All of these macroscopic fracture models are semi-empirical and require, for each application, a series of tests in order to correlate the model with the response of the test article. As they do not address, but rather by-pass, the micromechanical complexities in the crack extension process, the attempted generalizations of the models in regard to, e.g., stacking order or laminate dimensions, have not been fruitful.

A simple challenge to the validity of classical concepts is presented in Figure 24, showing a laminate with a transverse notch and unidirectionally oriented fibers. Fracture mechanical reasoning would idealize this laminate into an orthotropic plate with smeared homogeneity and, under static tensile load, expect a crack extension in the direction of the notch. In actuality the laminate behaves very differently. Emanating from the notch tips, cracks developing normal to the notch direction progress to the point of complete separation of the laminate with no growth in the notch direction at all.

In the case of fatigue loaded multidirectional specimens the resulting damage in the vicinity of holes or notches is considerably more complicated. Emanating from the notch tip or from the most highly stressed point on the periphery of the hole, cracks develop eventually in the fiber direction of each of the plies which increase in density and are followed by fiber ruptures, macrocracks and delaminations. Figure 25 and Figure 26 show examples of the damage zones at a notch tip and around a circular hole, respectively. It is difficult to conceive that this complex state of damage can be characterized by one or two empirically determined parameters. The problem assumes an even more challenging dimension when the holes are filled with mechanical fasteners and the damage state is affected by both bearing pressure and notch sensitivity.

7. Conclusion

Evidently, the issue of damage mechanics is of inordinate complexity and little tangible progress has been made so far. The remaining volume of work seems to be overwhelming and the question is valid whether the effort is worth the gain. The Institute for Structural Mechanics has adopted an affirmative position since, without the mastery of damage mechanics, the potential of composite construction cannot be fully exploited. Considering the highly competitive international market, the consequences of failing would be so grave that a relaxed stance in this matter can hardly be afforded.

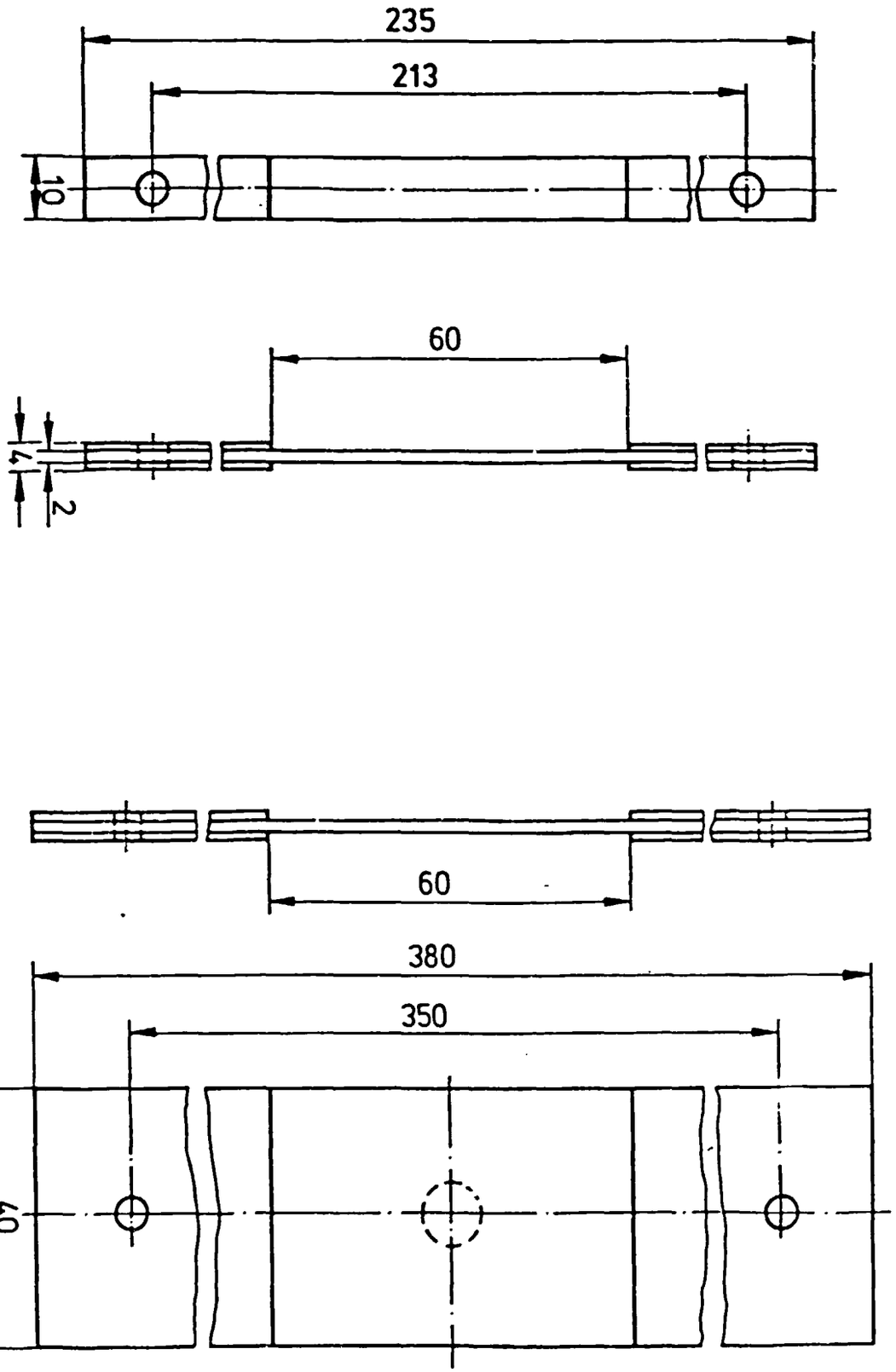

Fig. 1

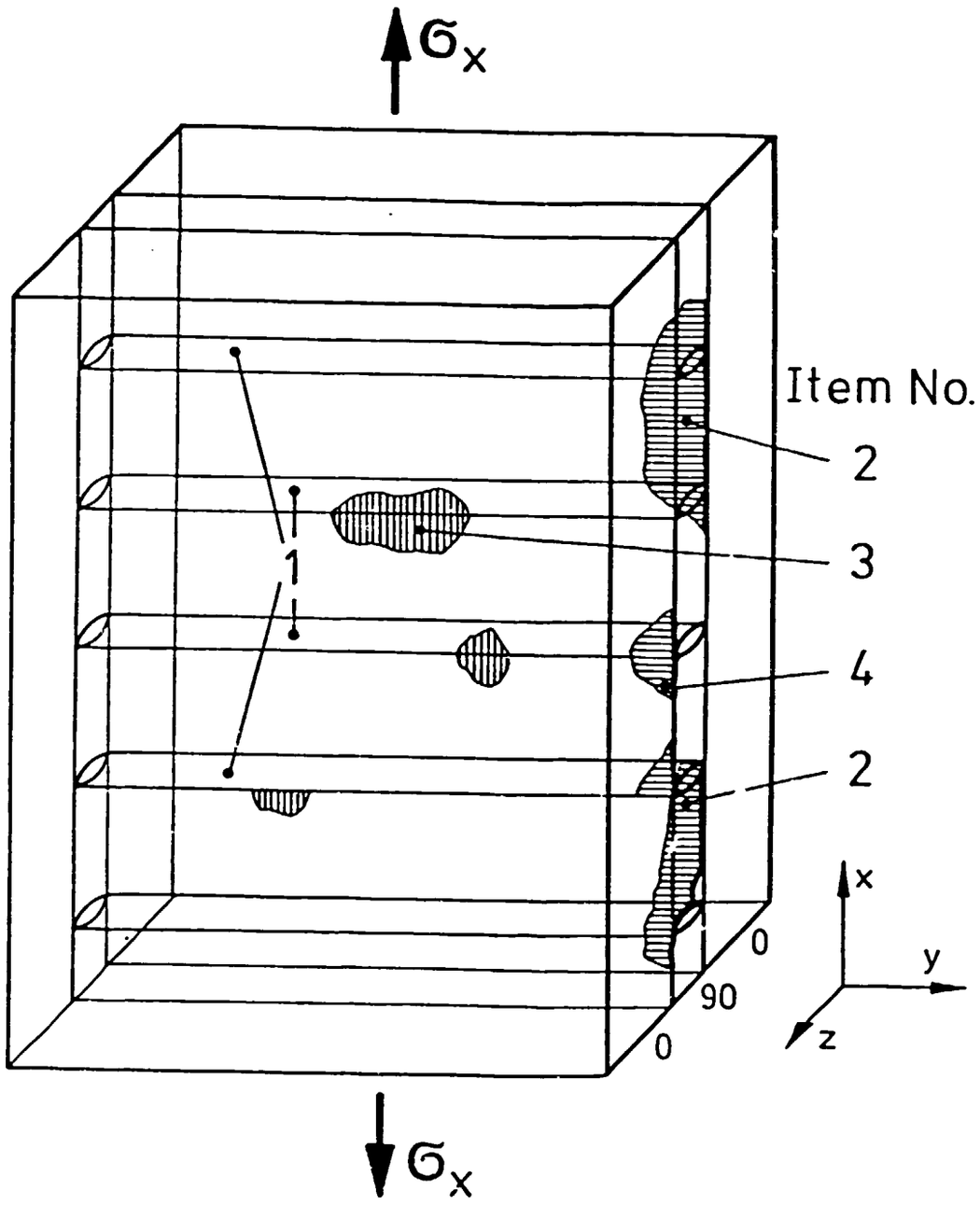

Fig. 2

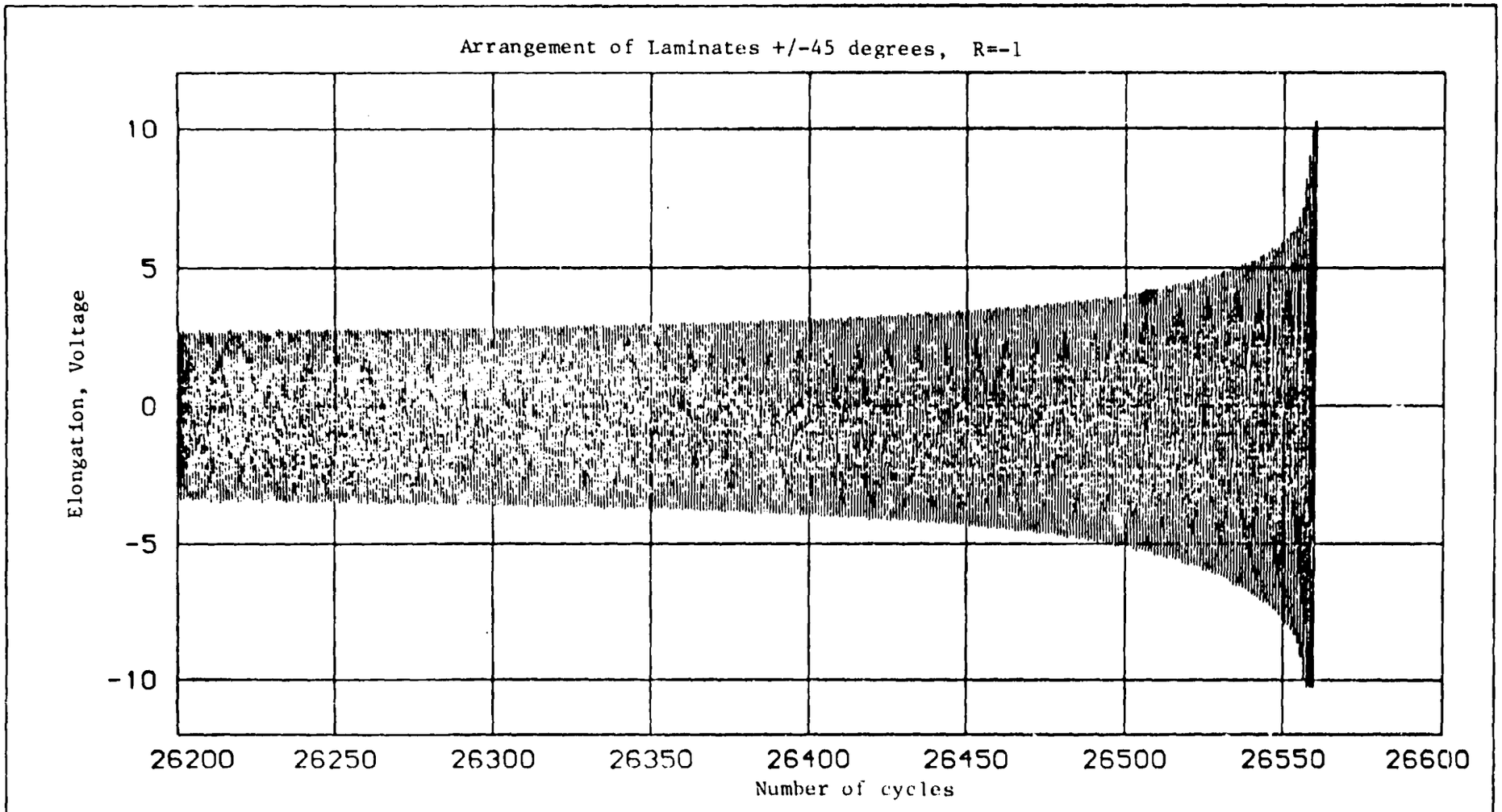

	Elongation during testing TIFGA8	131/13

Fig.3

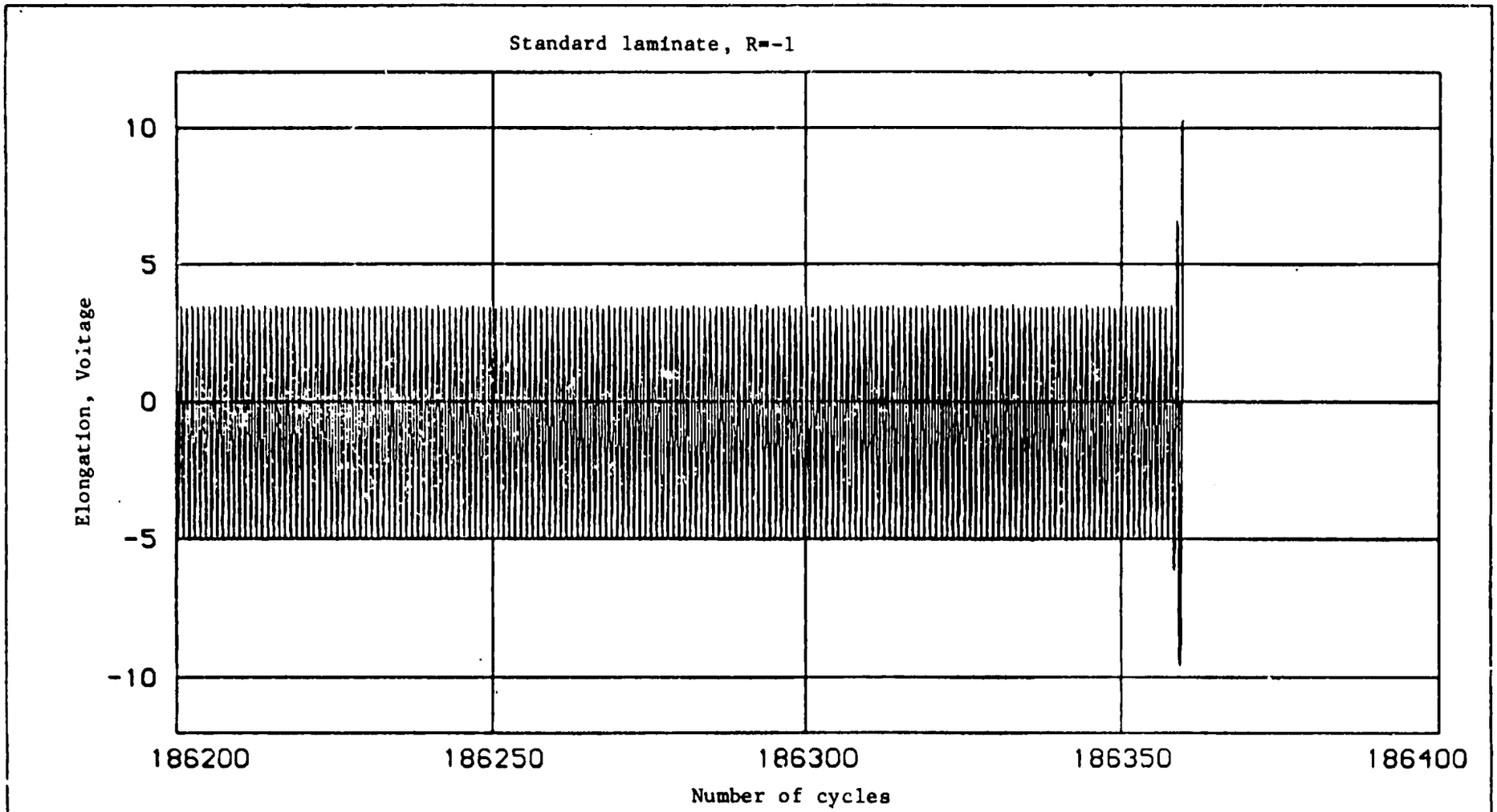

	Elongation during testing TFGUNO	131/13

Fig. 4

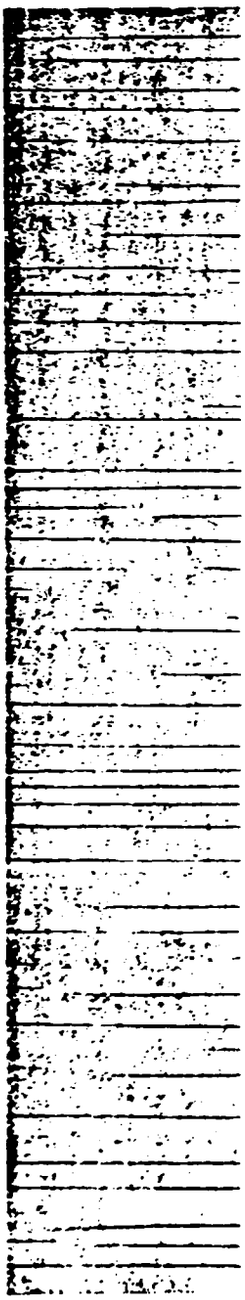

Fig. 5

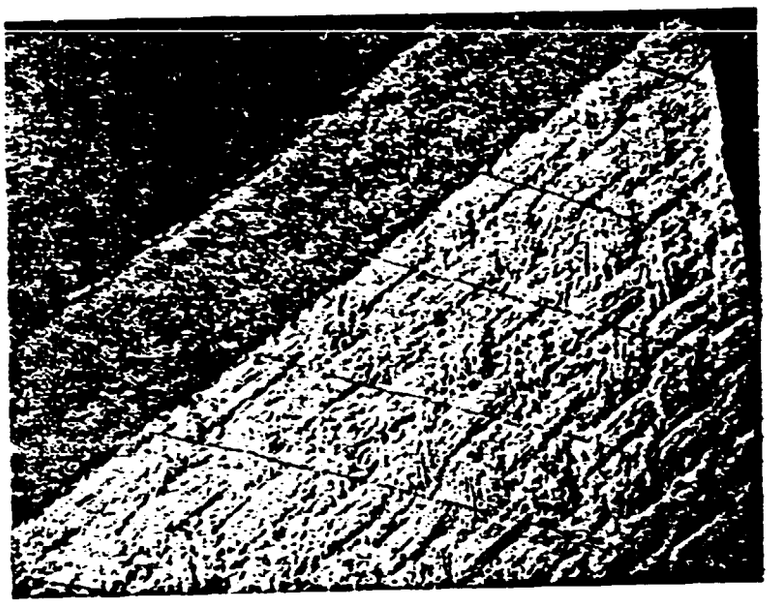

Surface and Cross Section (30x)

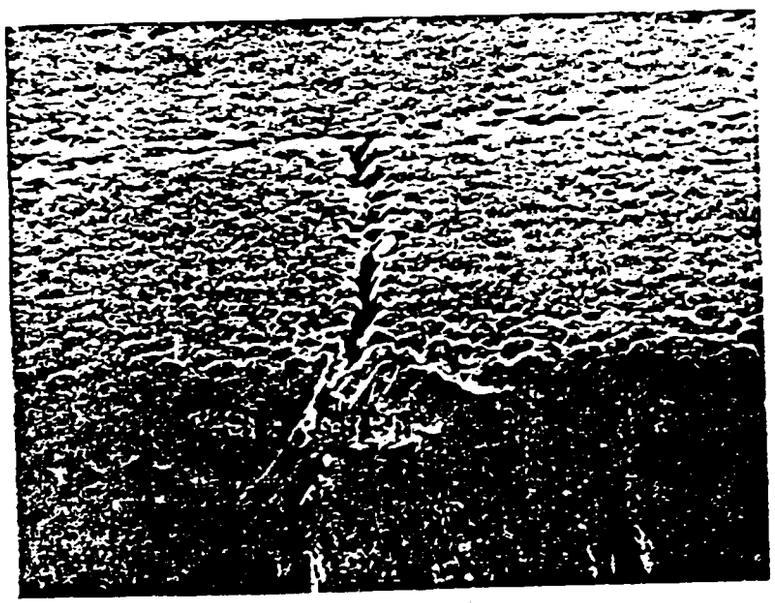

Cross Section (400x)

Sample of T3T F 178 After 1170 Thermal Cycles

Fig. 6

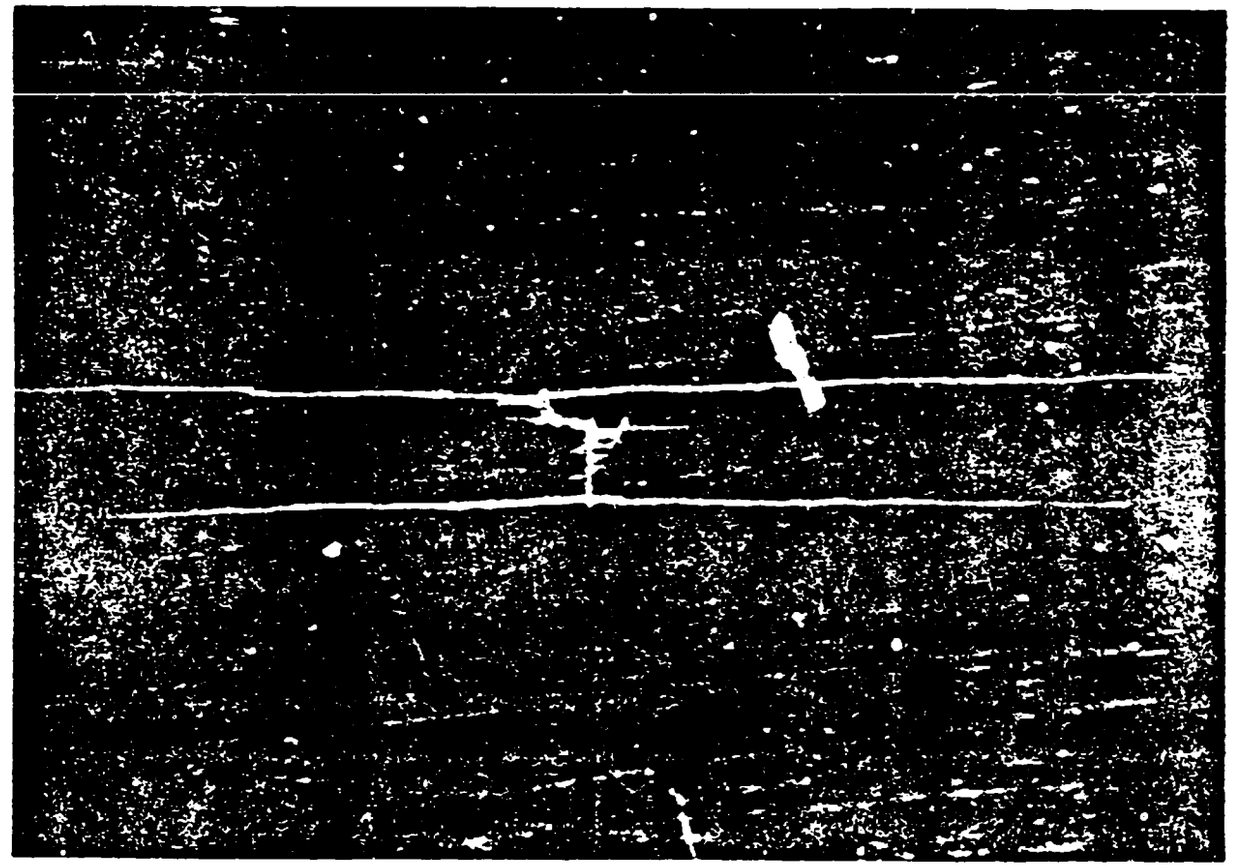

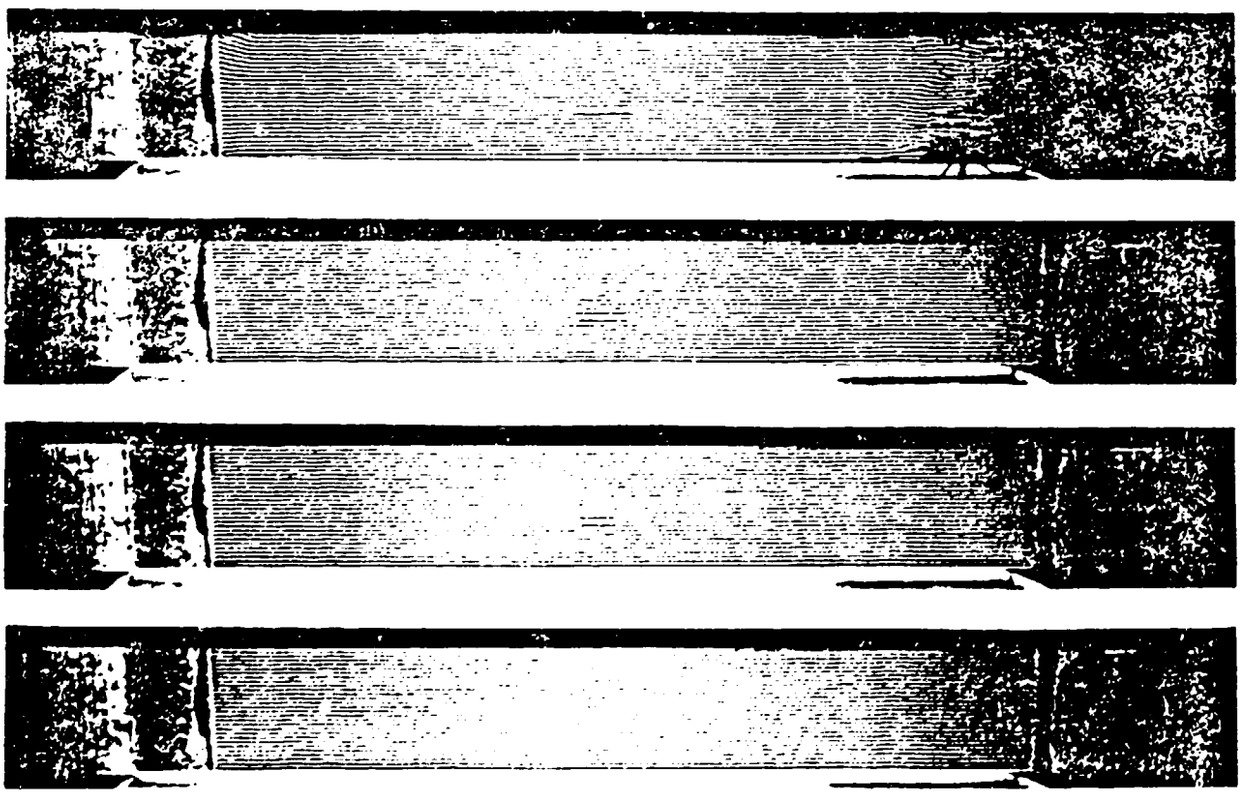

Fig. 7

Prior to Cycling 186x

After 3480 Thermal Cycles 186x

Typical Fracture Areas of 914C - Specimens Before and After Thermal Cycling

Fig. 8

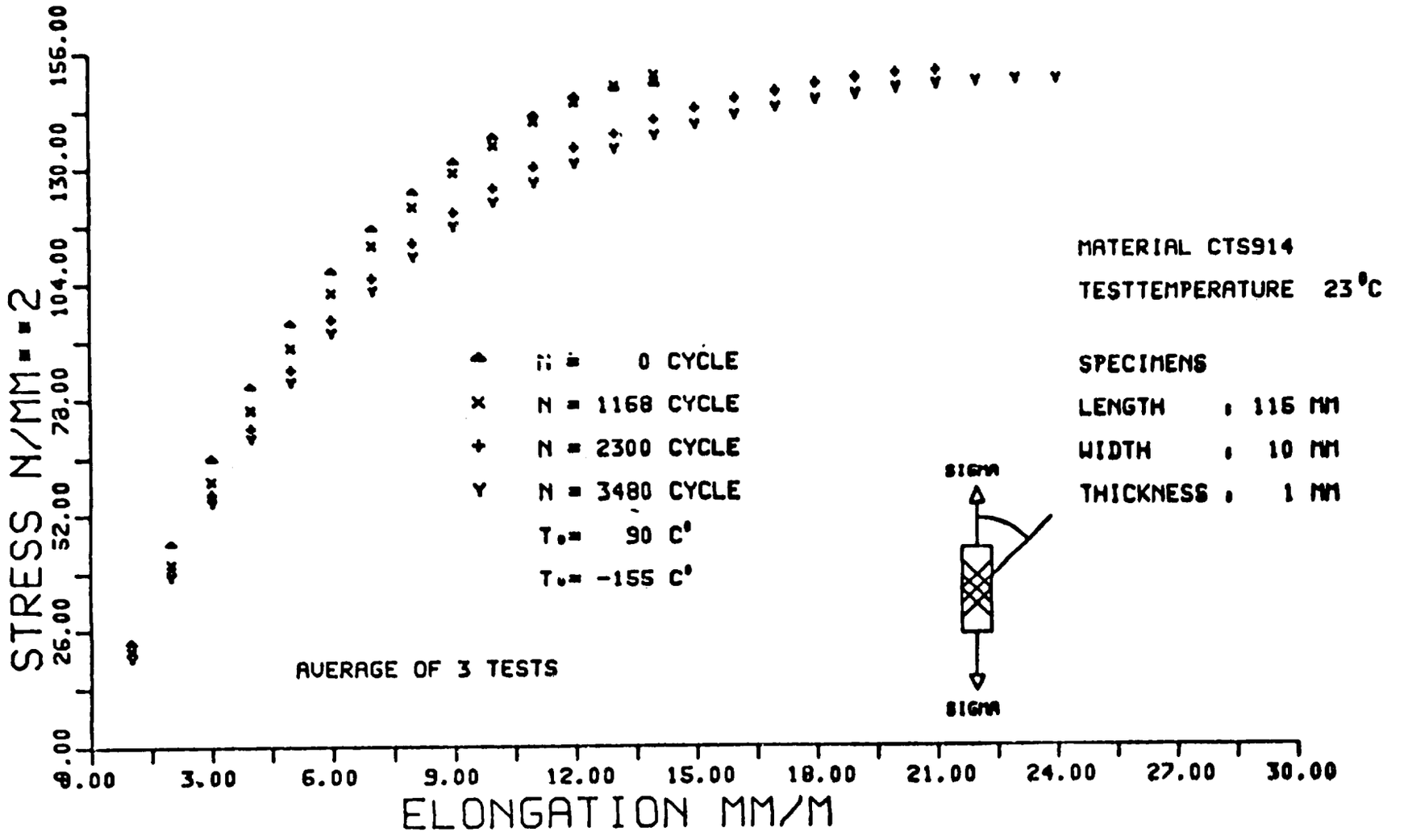

Stress-Strain Slope From Tension on ± 45° CRP After Thermal Cycling

Fig. 9

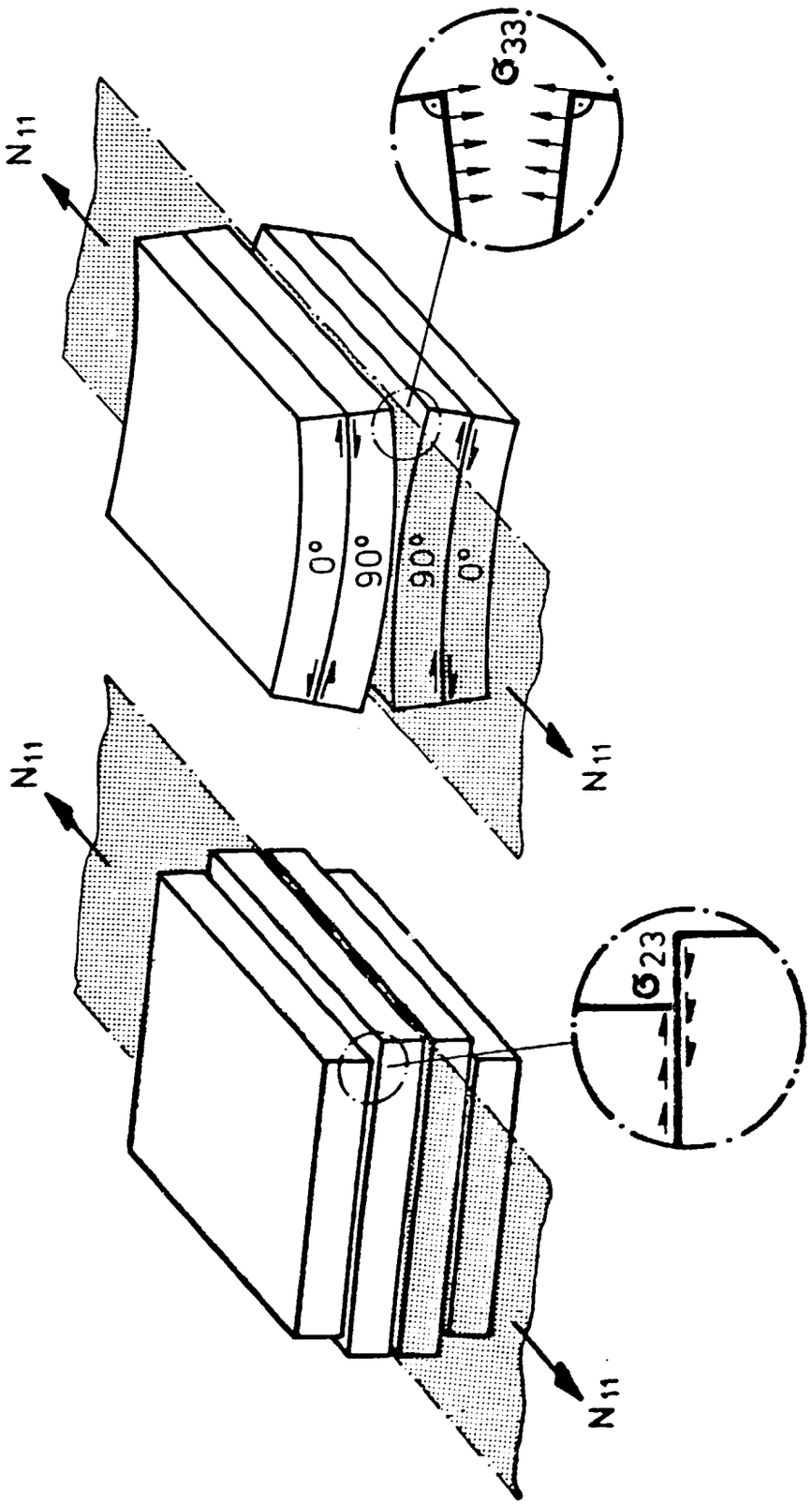

Fig. 10

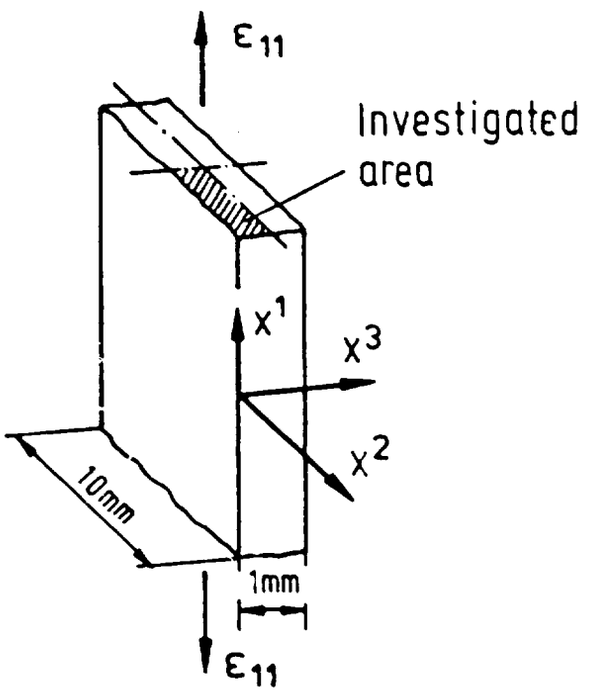

Stacking sequences

——— [90°,-45°,+45°,0°]s

– – – [0°,-45°,+45°,90°]s

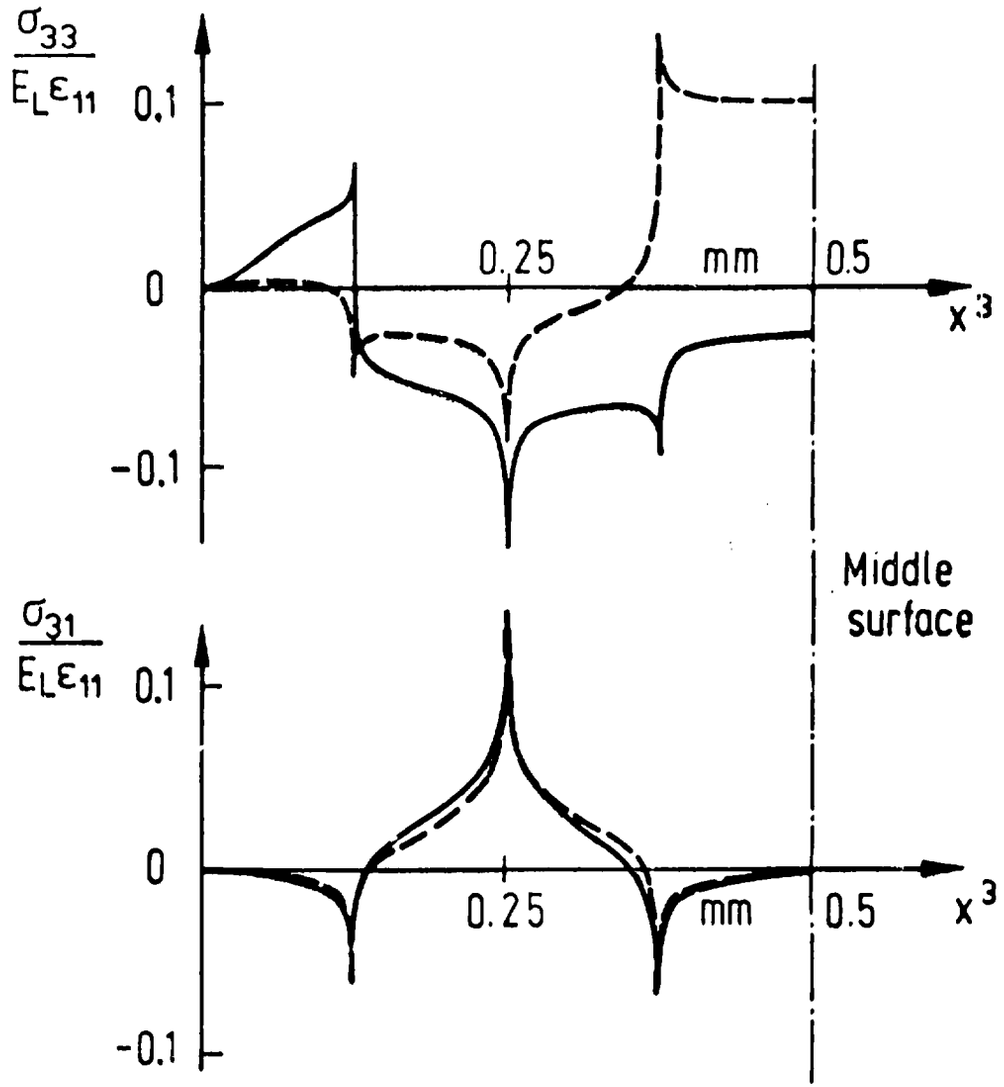

Free edge stresses under axial tension for different stacking sequences of a laminate

Fig. 11

Fig. 12

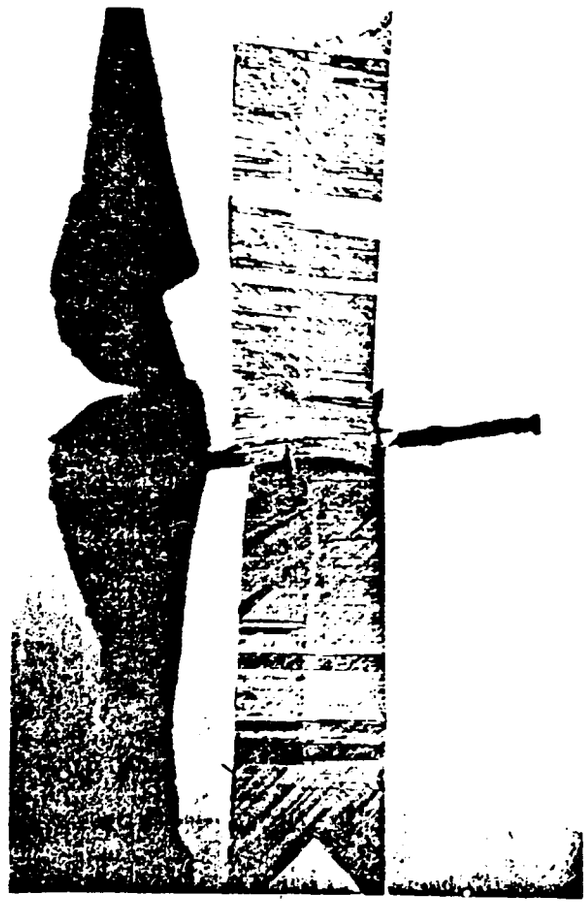

Fig. 13

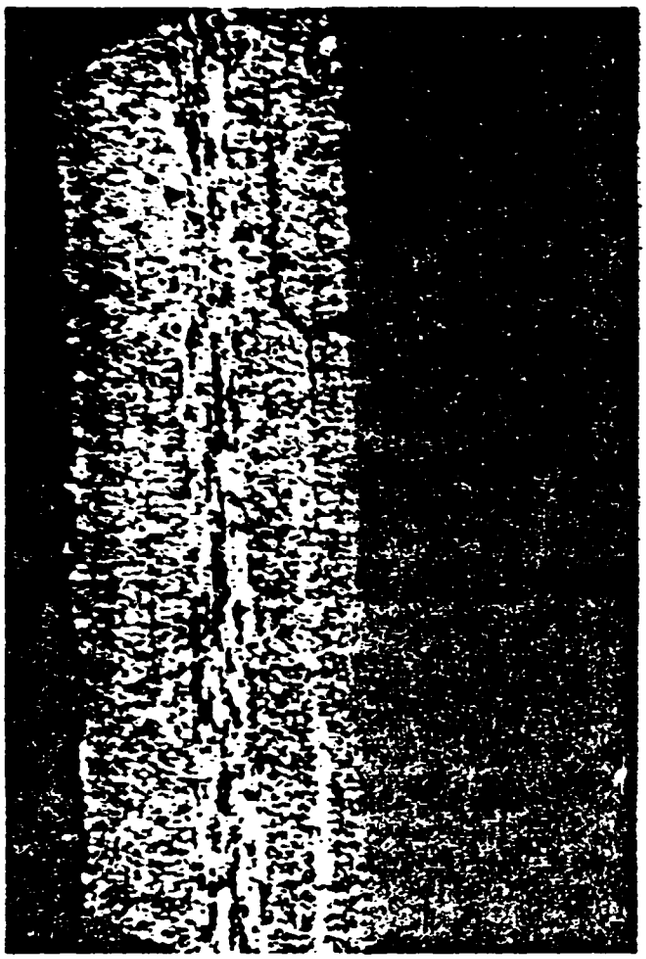

Fig. 14

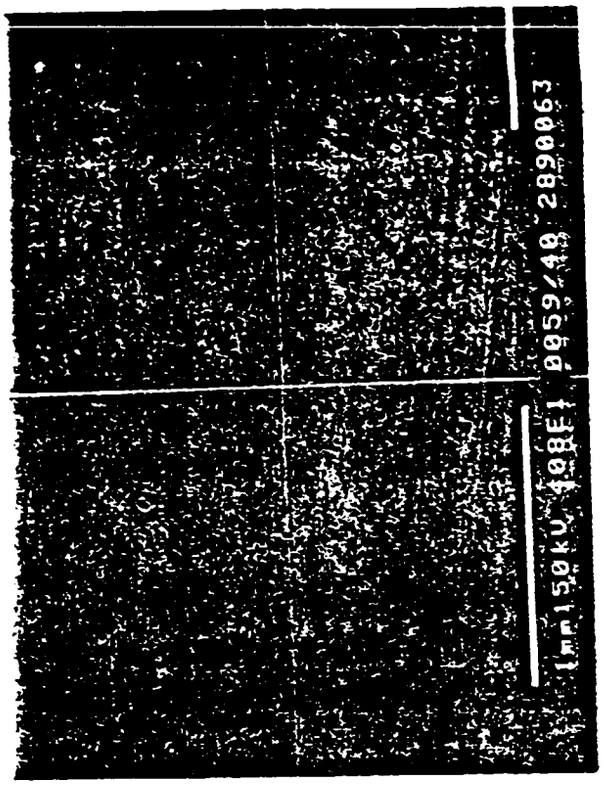
1mm 15.0kV 10BEI 0059/48 2890063


10µm 15.0kV 5.79E3 0062/48 8E


15.0kV 10BEI 0011/48 2890063

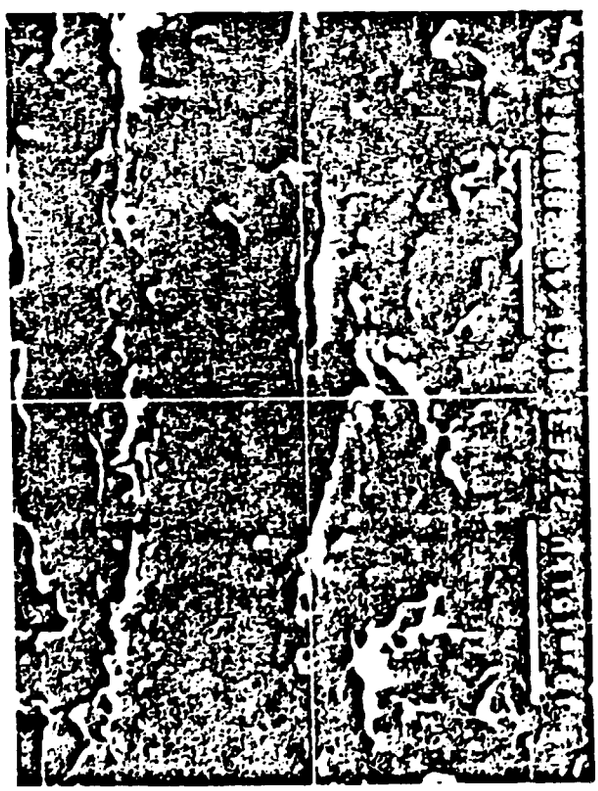

Fig. 15

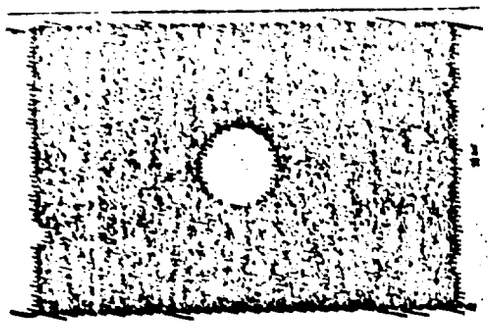

0 N/mm²

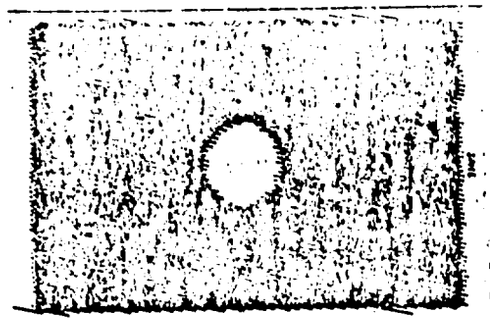

700 N/mm² (744)

725 N/mm² (790)

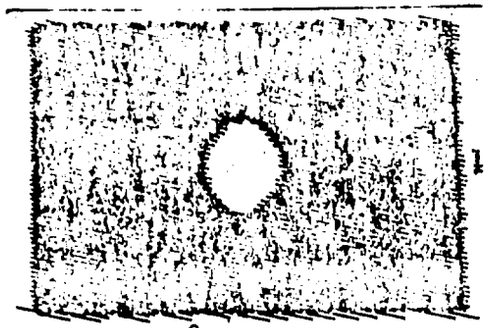

750 N/mm² (817)

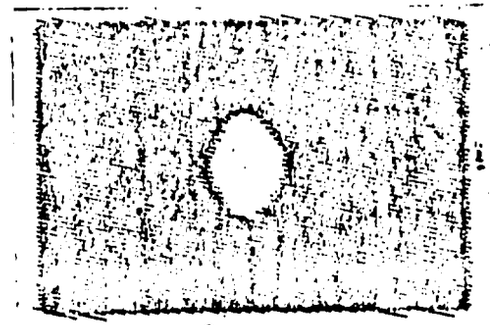

775 N/mm² (1142)

20mm

CFRP sample 214/6 thickness: 2 mm

Layer structure: $(0^{o}_{2},+45^{o}, 0^{o}, 90^{o})_{S}$

Delamination in middle layer of the sample - stat. pressure load

Fig. 16

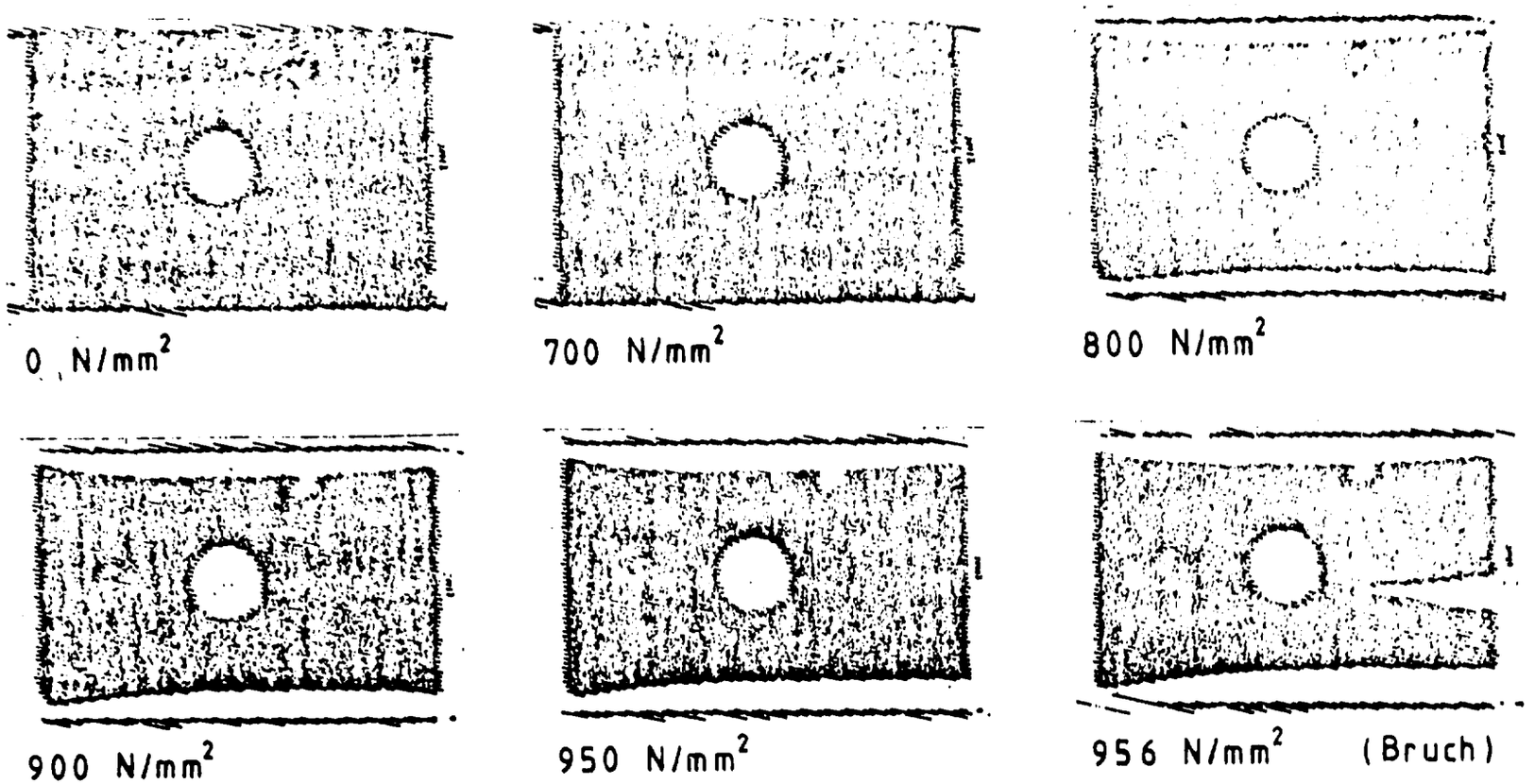

CFRP-sample 214/7 thickness 2 mm

Layer structure: $(0^o_2, +45^o, 0^o_2, -45^o, 0^o, 90^o)_S$

Delamination in middle layer of the sample - stat. pressure load

Fig. 17

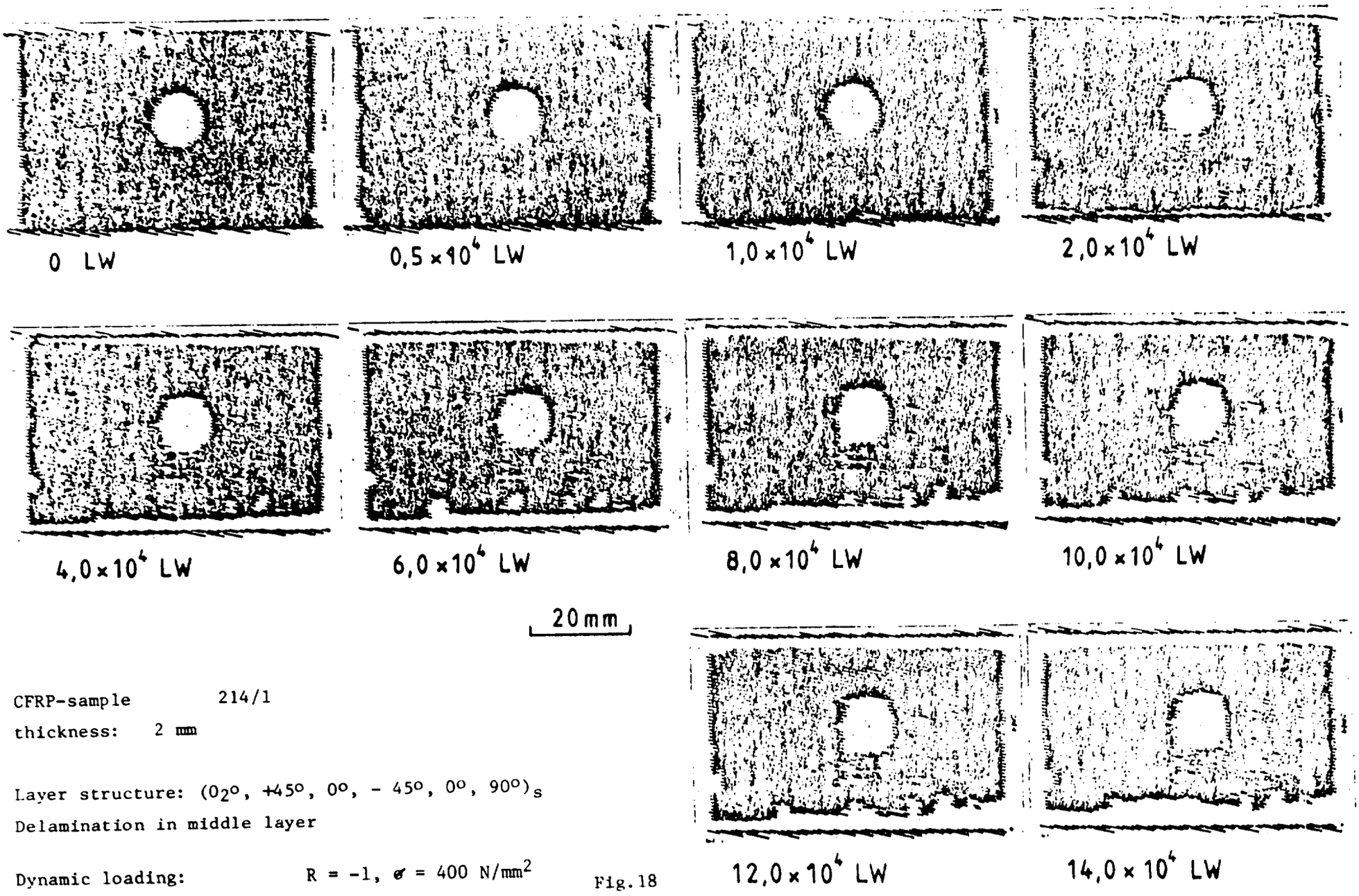

CFRP-sample 214/1

thickness: 2 mm

Layer structure: $(0_2^o, +45^o, 0^o, -45^o, 0^o, 90^o)_s$

Delamination in middle layer

Dynamic loading: R = -1, σ = 400 N/mm^2

Fig.18

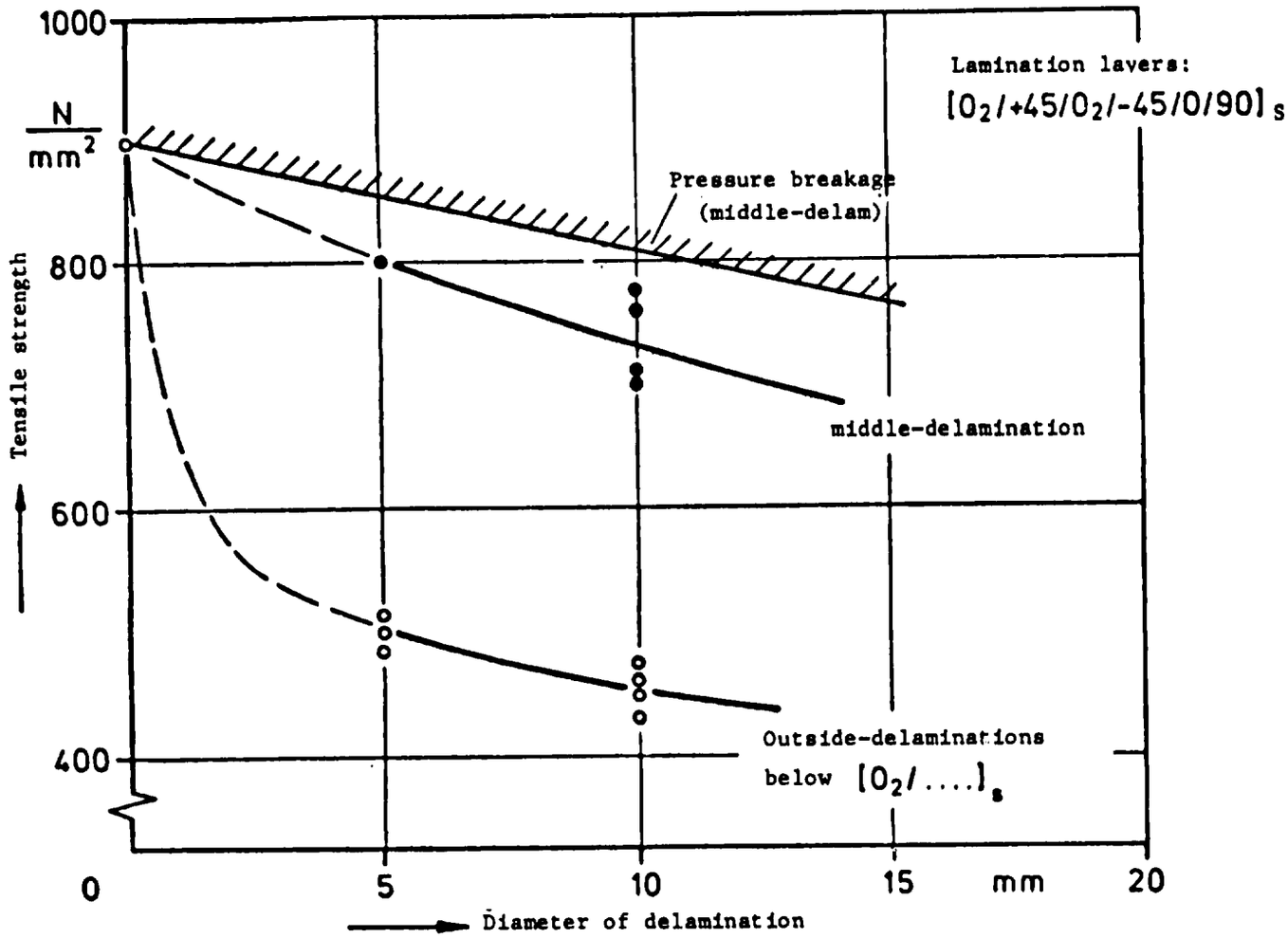

Influence of the delamination-amounton the spreading of delamination under compression loading.

Fig. 19

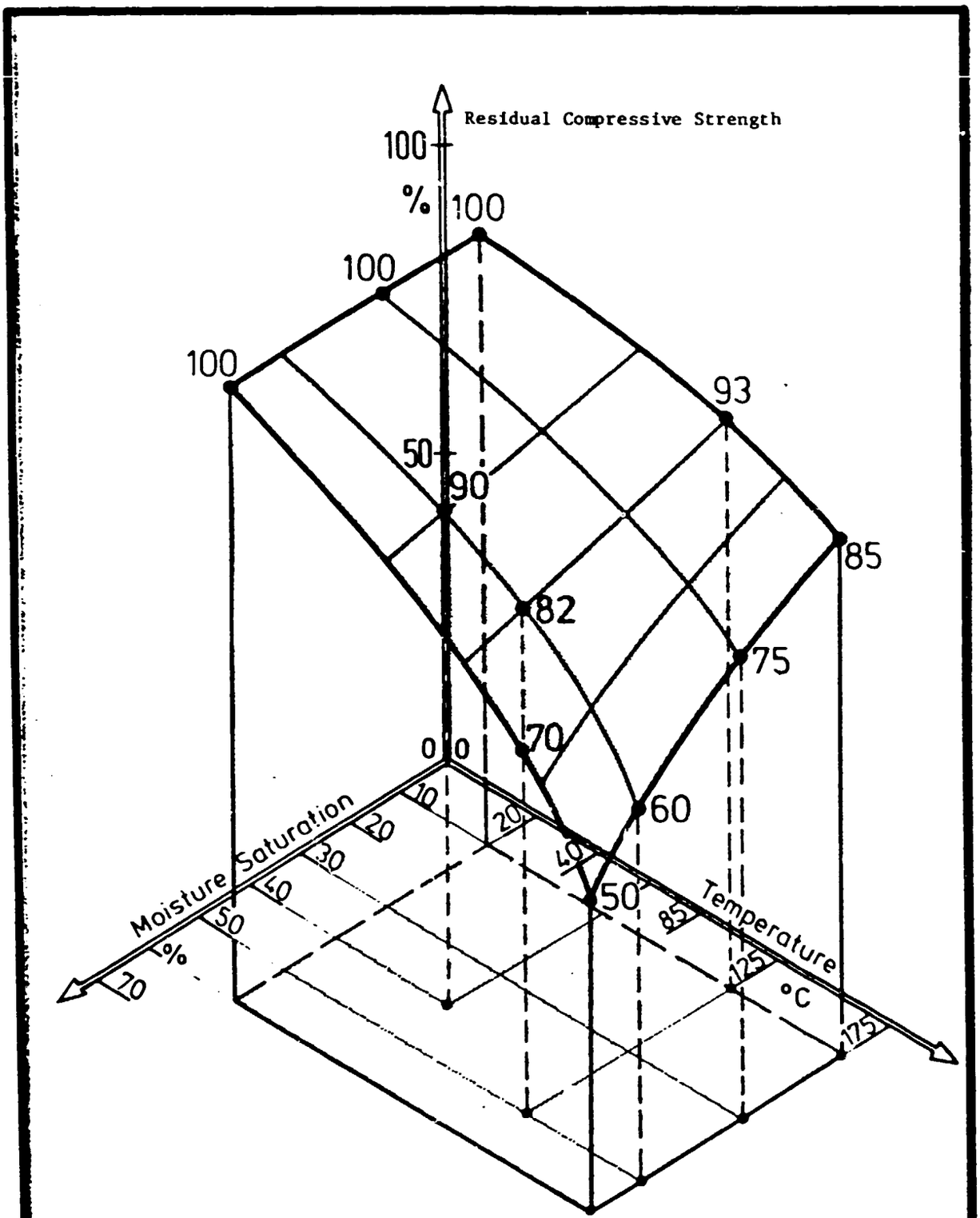

	Degradation of Compressive Strength	131 - 14

Fig. 20

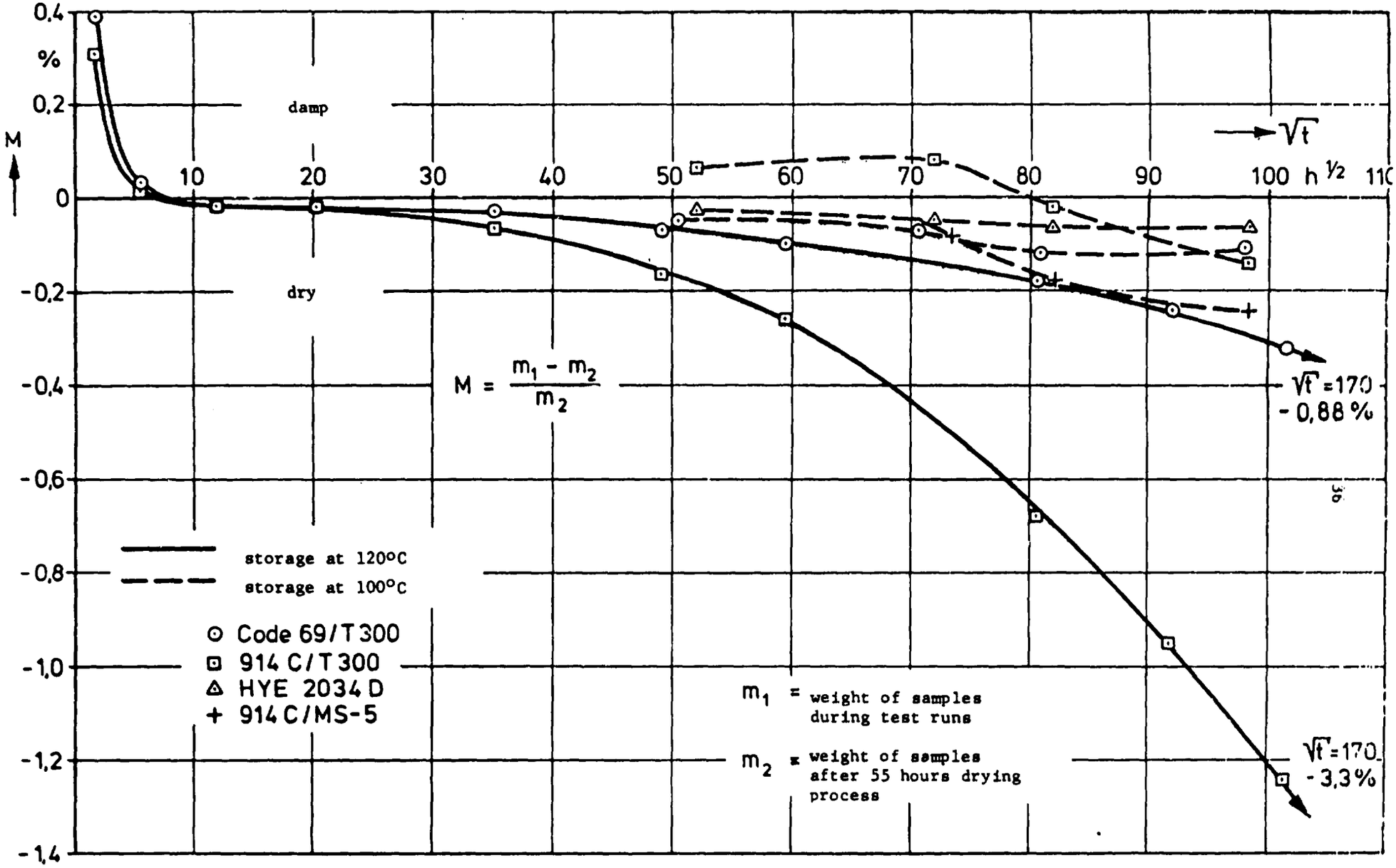

Weight loss of CFRP-laminates caused by outgasing during long time testing at 100oC and 120°C

Fig. 21

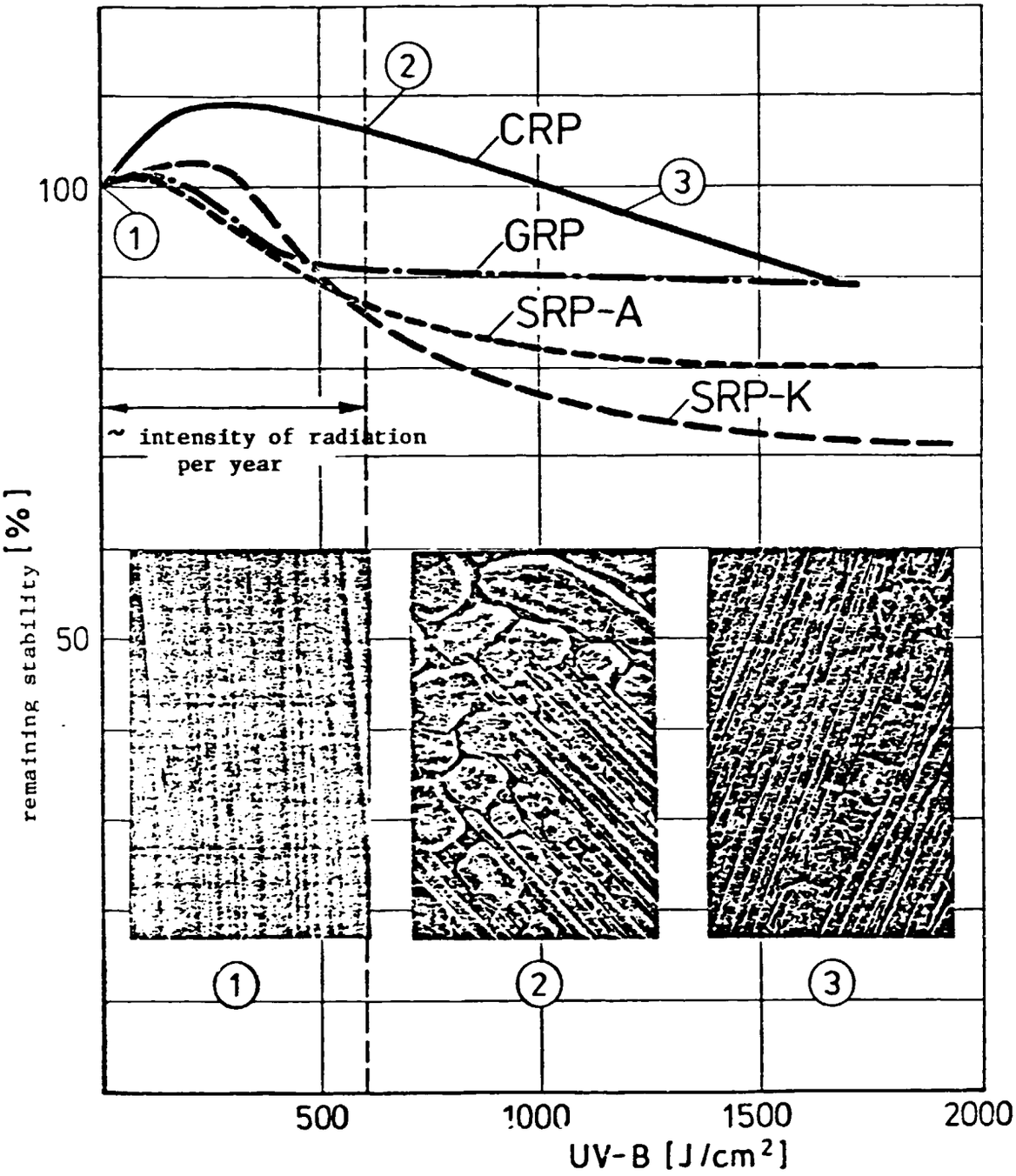

Matrix: Aliphatic EP-resin
cycloaliphatic amine

Hardness: 1,5h 90°C, 6h 100°C

Stiffness: Fibre textile

Degradation caused by UV-B-radiation

Fig. 22

CFK-Proben nach Temperatur- und Feuchteinwirkungen

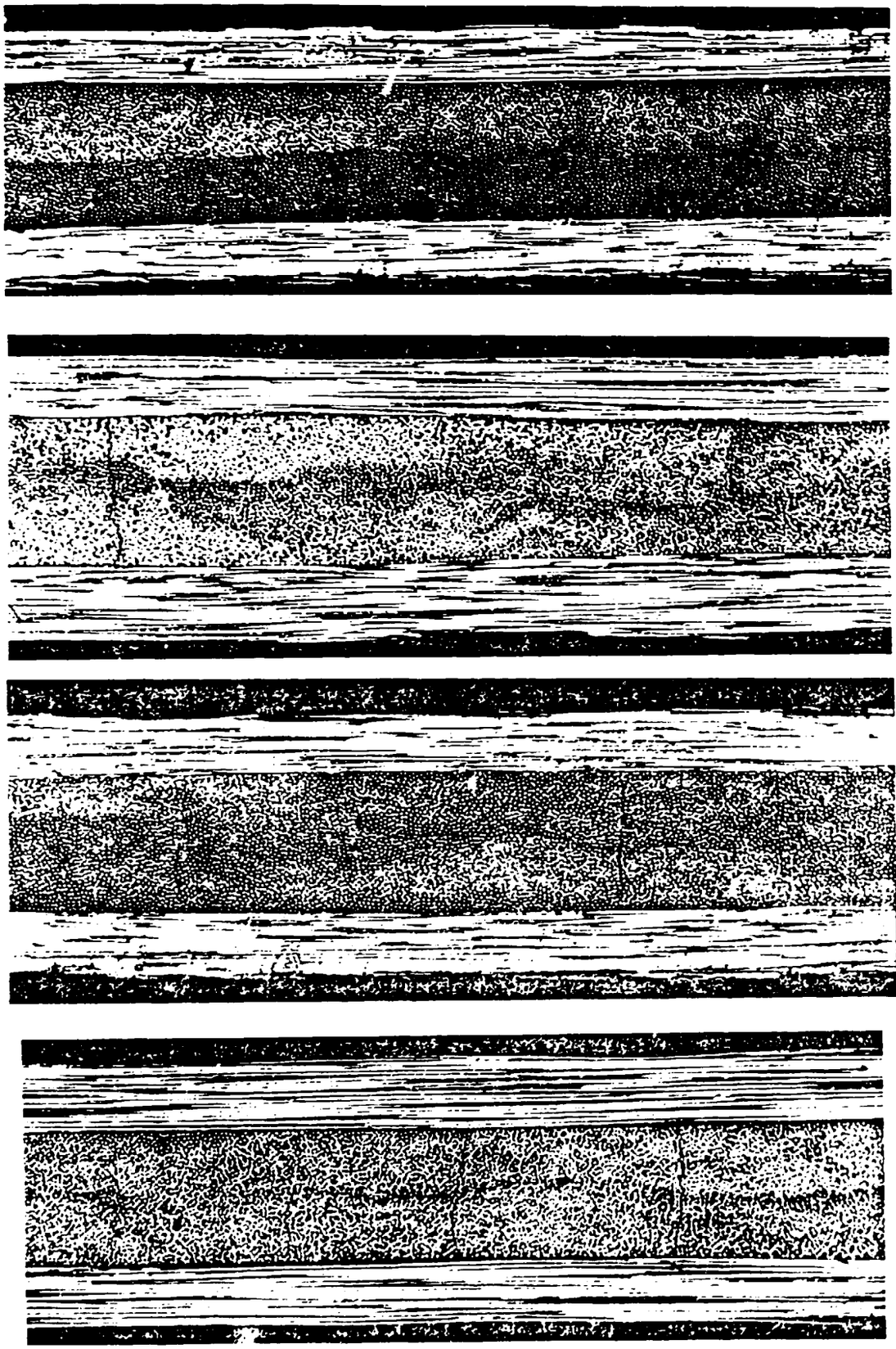

keine Risse bei:

40°C, 93%

120°C 93%

120°C, 0%

40°C, 0%

(1 R:p)

-55°C, 93%

(2 Risse)

-55°C, 0%

(4 Risse)

V = 100 : 1

Fig. 23

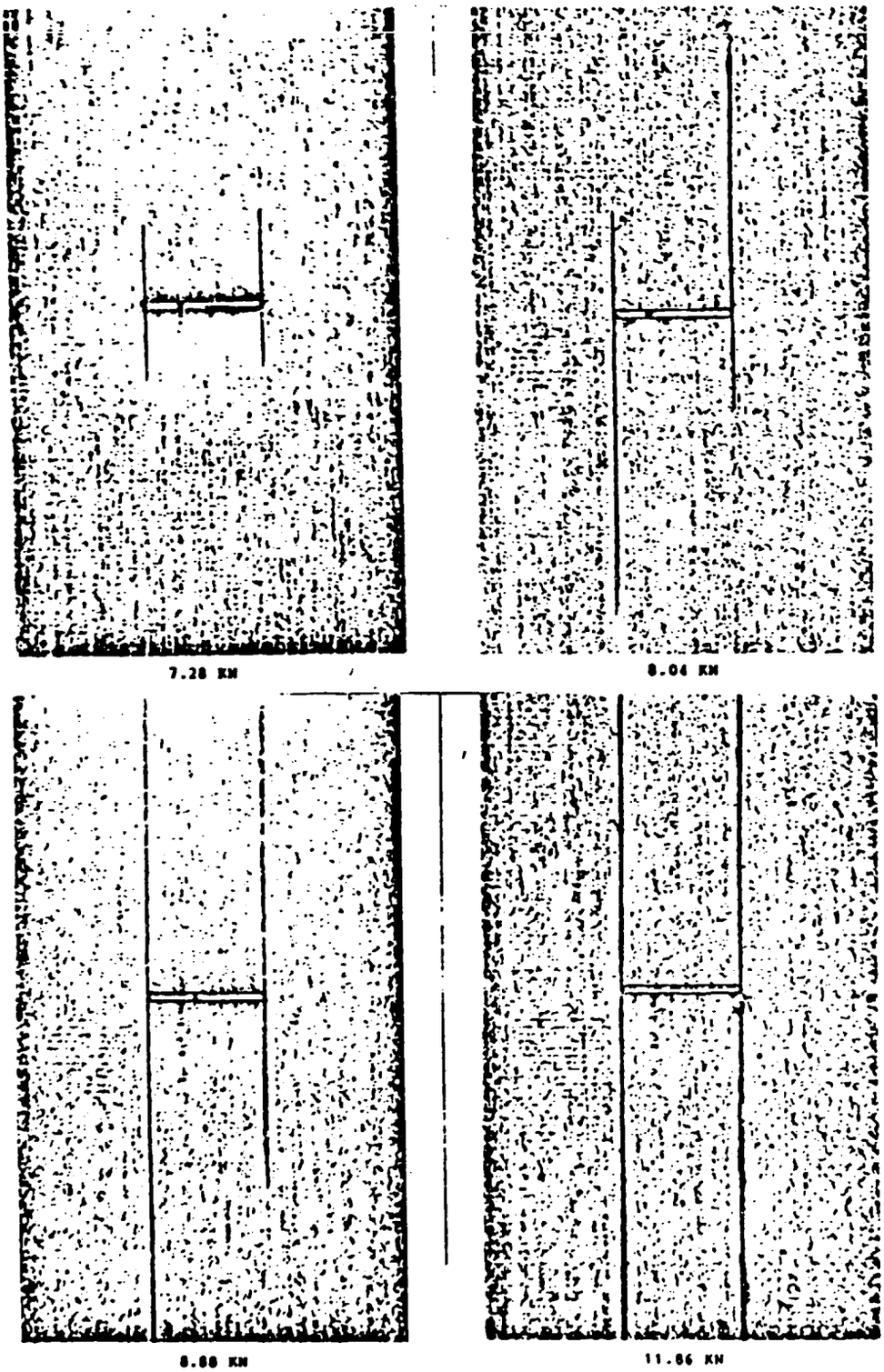

Crackpropagation in a CFRP sample with internal notch

Layerstructure: $(0^{o})_{8}$, width of sample: 25 mm

Fig. 24

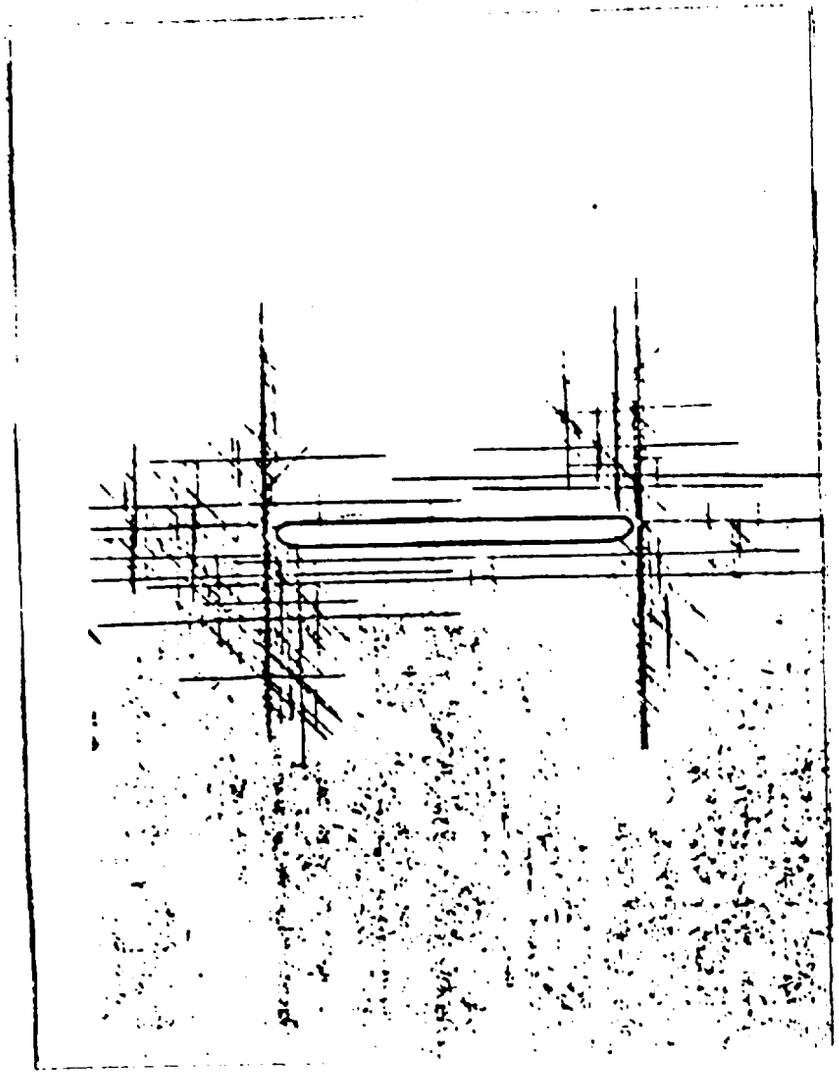

10,20 kN

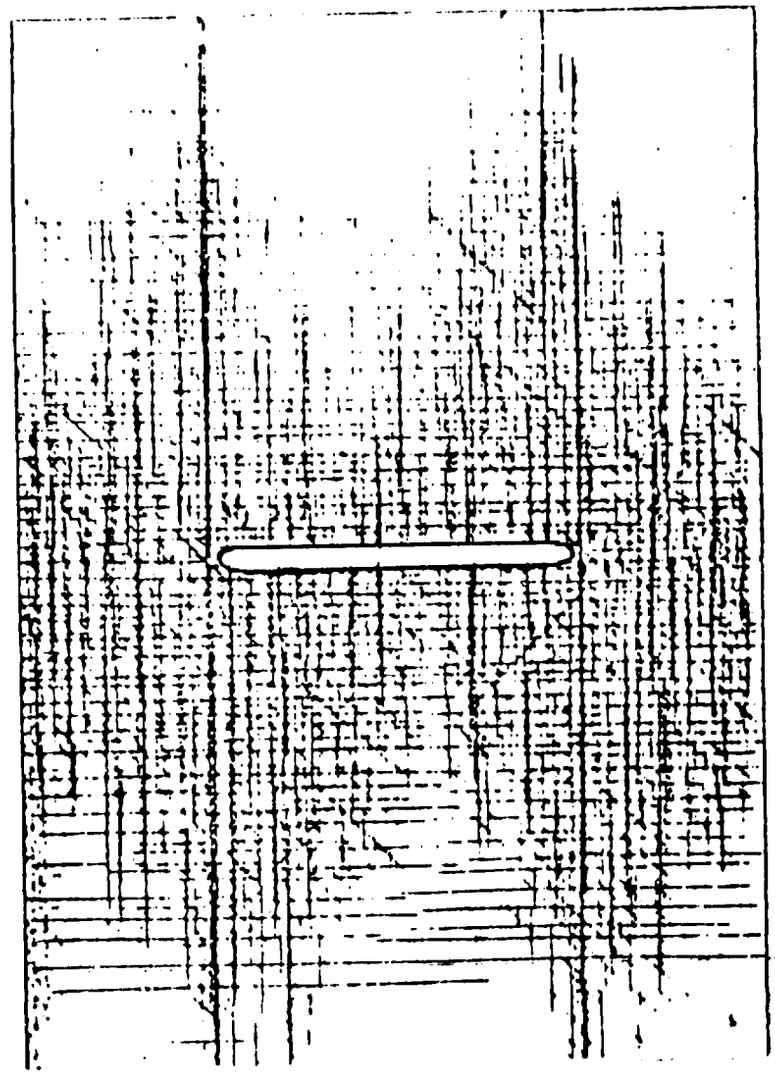

13,10 kN

Crackpropagation in a CFRP-sample with internal notch

Fig. 25

structure of laminate: $[0_2/+45/0_2/-45/0/90]_S$

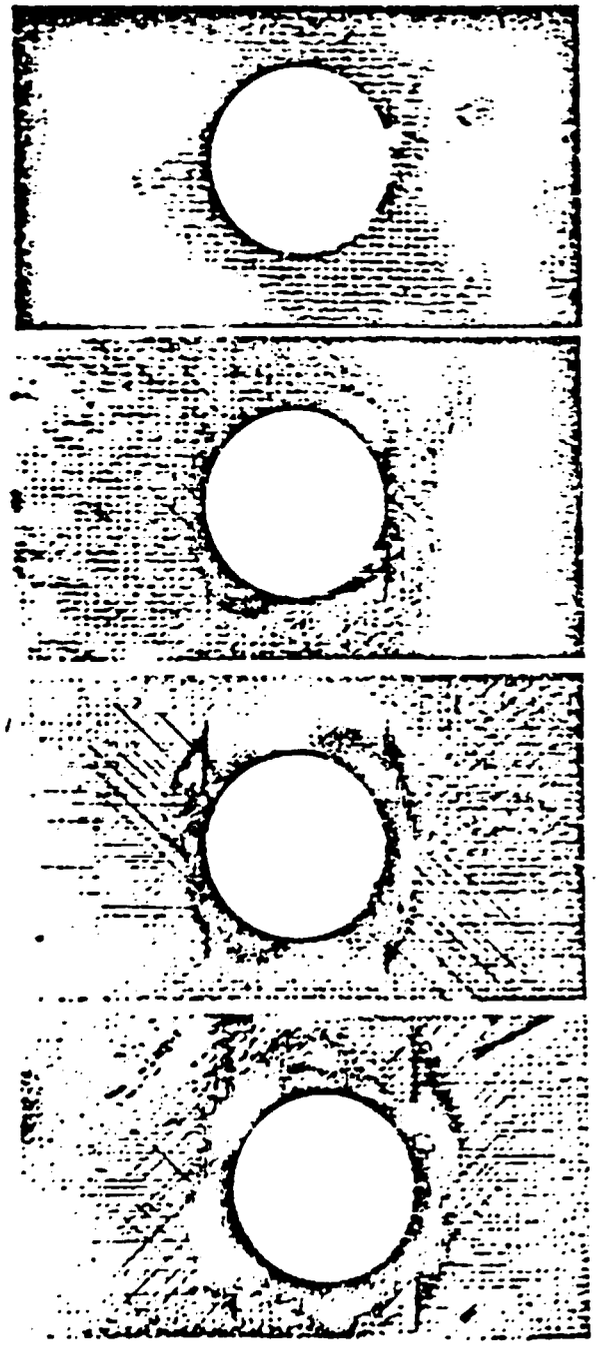

Fig. 26